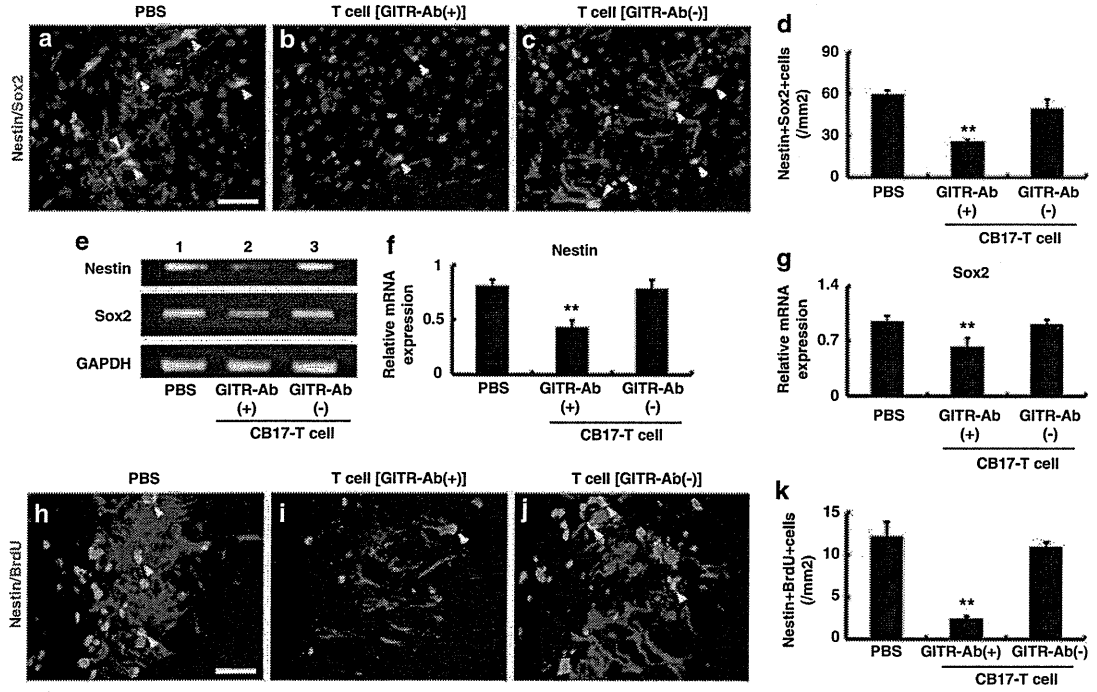

Figure 6 Effects of administration of T cells triggered by GITR on survival/death of neural stem/progenitor cells. (**a–d**) Co-expression of nestin (red) and Sox2 (green; arrowheads) was investigated 7 days after stroke in SCID mice, which were injected with T cells. Compared with the PBS-injected control mice (**a**), mice treated with GITR-stimulated T cells showed significantly less nestin/Sox2-positive cells (**b**), whereas mice treated with non-stimulated (control-IgG stimulated) T cells showed no difference compared with the control (**c**). (**d**) $n=6$, 3 and 3 for PBS-, GITR-stimulated T cell and non-stimulated T cell-treated groups, respectively. Expression of nestin or Sox2 detected by conventional RT-PCR in the ischemic tissue on day 7 (**e**) was significantly decreased after treatment with GITR-stimulated T cells (**e**: second lane) compared with control (PBS; **e**: first lane) or non-stimulated T-cell treatment (**e**: third lane; **f**: nestin; **g**: Sox2). (**f** and **g**) $n=5$ for each experimental group. (**h–k**) The number of proliferated neural stem/progenitor cells evaluated with anti-nestin (red) and anti-BrdU (green) antibodies (arrowheads) on day 7 was significantly decreased after treatment with GITR-stimulated T cells (**i**), compared with control (**h**) or non-stimulated T cell-treatment (**j**). Quantitative analysis confirmed the decreased number of nestin/BrdU-positive cells in GITR-stimulated T-cell-treated mice, compared with the other two groups (**k**; $n=5$ for each experimental group). $^{**}P<0.01$ *versus* PBS- or non-stimulated T cell-treated (GITR-Ab(−)/CB-17 T cell) mice. (**a** and **h**) Scale bar: 50 μm

Effects of GITR-stimulated T cells on survival/death of neural stem/progenitor cells. As the ischemic insult enhanced the expression of GITR on infiltrated $CD4^+$ T cells (Figures 1–3) and GITR triggering disrupted iNSPCs in poststroke mice (Figure 5), we next investigated whether GITR-triggered, activated $CD4^+$T cells could affect survival/death of iNSPCs. Activation of $CD4^+$T cells by ligation of GITR has been reported previously,[17] and we also confirmed enhanced expression of GITR on $CD4^+$T cells by GITR–Ab (DTA-1; see Figure 8d; lanes 3, 4). Initially, to confirm infiltration of the administered T cells into the ischemic area, T cells extracted from the green fluorescence protein-transgenic (GFP-Tg) mice were injected into SCID mice 2 days after stroke as described previously.[7,20] Five days after administering, the GFP-positive T cells migrated selectively into the infarction area of the poststroke brain (Supplementary Figure 2). Next, we injected T cells of CB-17 mice (either stimulated or non-stimulated by GITR–Ab) as described above, and examined the expressions of nestin/Sox2 double-labeled cells 5 days after injection by immunohistochemistry (Figures 6a–d). In accordance with our previous report,[8] poststroke SCID mice with PBS injection (control) expressed a greater number of nestin/Sox2-positive iNSPCs than CB-17 mice (compare Figure 6d with Figure 5h). The administration of GITR-stimulated T cells significantly decreased the number of nestin/Sox2 cells (Figures 6b and d; $P<0.01$), whereas non-stimulated T cells had no significant effect (Figures 6c and d). These findings were confirmed by conventional RT-PCR analysis (Figure 6e). Relative expressions of both nestin and Sox2 were attenuated by administration of GITR-stimulated T cells but not by non-stimulated T cells (Figures 6f and g). The proliferation of iNSPCs was also evaluated by labeling of nestin-positive cells with bromodeoxyuridine (BrdU), as per a previous report.[8] GITR-stimulated T cells significantly decreased the number of BrdU-labeled nestin-positive cells compared with PBS treatment as a control (Figures 6i and k; $P<0.01$), whereas non-stimulated T cells had no significant effect (Figures 6j and k). These findings indicate that GITR-triggered, activated $CD4^+$T cells, but not non-stimulated T cells, affect survival/death of iNSPCs after stroke.

***In vitro* effects of TNF-α and Fas ligand on apoptosis of neural stem/progenitor cells.** To determine how activated $CD4^+$T cells ligated by GITR affect survival/death of iNSPCs, a cell death assay was performed using cultured neurospheres consisting of iNSPCs (Figure 7a). It is well known that some neural stem/progenitor cells undergo

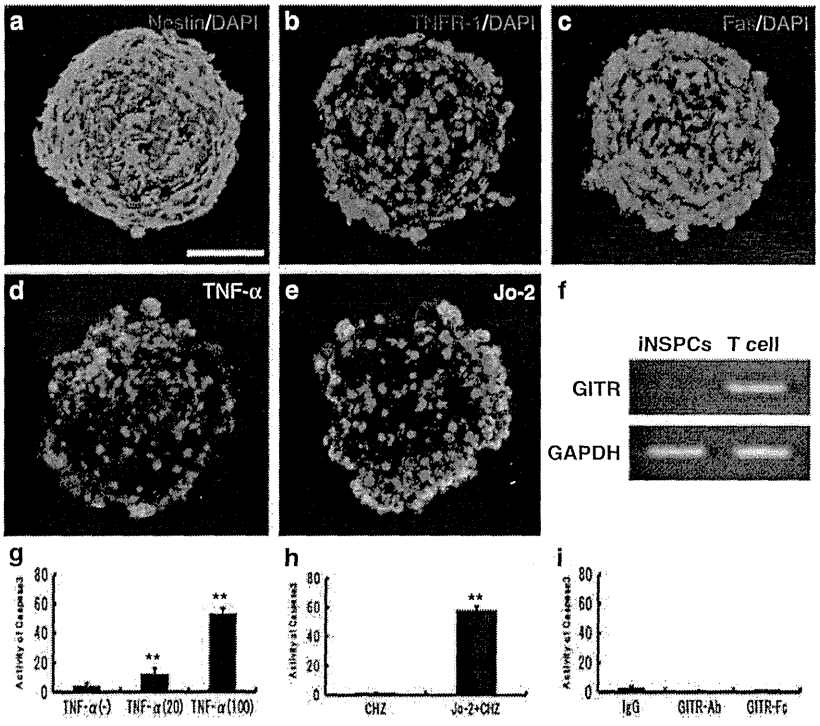

Figure 7 *Involvement of death factors in apoptosis of iNSPCs neurospheres. In neurospheres obtained from the ischemic areas of poststroke mice, nestin (green;* **a**), TNFR-1 (red; **b**) and Fas (red; **c**) were virtually observed (DAPI, blue). Incubation with TNF-α (**d**) or Jo-2 (**e**) induced collapse of cell clusters with expression of a marker of apoptotic cell death, anionic phosphatidylserine visualized with Annexin V staining (green). (**f**) GITR was not expressed on iNSPCs neurosphere. (**g**) Incubation with TNF-α increased the activity of caspase-3 in neurospheres in a dose-dependent manner. Jo-2 also increased the activity (**h**), but neither GITR–Ab (DTA-1) nor GITR–Fc activated caspase-3 on the neurospheres (**i**). (**a** and **d**) Scale bar: 100 μm. (**g**–**i**) $n=3$ for each experimental group. $^{**}P<0.01$ *versus* control groups (**g**: without TNF-α; **h**: CHZ without Jo-2). No significant difference was found among the groups (**i**)

apoptosis, with expression of multiple cell death signals such as TNF receptor-1 (TNFR-1)[23] and Fas.[8] Consistent with these studies, we confirmed expression of TNFR-1 (Figure 7b) and Fas (Figure 7c) on iNSPC neurospheres. The neurospheres were incubated with Dulbecco's modified Eagle's medium (DMEM) containing TNF-α or agonistic Fas antibody (Jo-2) for 24 h, and their apoptosis was analyzed by Annexin V staining and active caspase-3 assay. As expected, TNF-α induced apoptosis of neurosphere cells (Figure 7d; green: Annexin V, red: PE). The activity of caspase-3 in the apoptotic neurosphere was increased dose dependently by TNF-α (Figure 7g). Jo-2 also induced apoptosis of neurospheres (Figure 7e), with a significant increase in caspase-3 activity (Figure 7h). Because iNSPCs neurosphere do not express GITR (Figure 7f), it is not likely that GITR signaling regulates death-receptor-induced apoptosis directly in iNSPCs. Accordingly, neither GITR–Ab nor GITR–Fc activated caspase-3 on the neurospheres (Figure 7i). These findings suggest that the death signaling pathway may be stimulated either directly or indirectly by activated $CD4^+$T cells ligated by GITR. Moreover, these results also prove that the triggering of GITR directly have no effect on apoptosis of iNSPCs.

Effect of GITR-stimulated Gld-T cells on survival/death of neural stem/progenitor cells. To assess the action of activated T cells, neurospheres were incubated with T cells (either GITR stimulated or non-stimulated) for 24 h (Figures 8a and b). Consistent with previous studies,[16,24] T cells stimulated by GITR–Ab showed upregulation of Fas ligand (FasL) expression (Figures 8c and d; lanes 3 and 4) as well as GITR expression (Figure 8d; lanes 3 and 4). Annexin V staining showed that neurospheres coincubated with GITR-stimulated T cells underwent apoptosis (Figure 8a), but those with non-stimulated T cells did not (Figure 8b). This result strongly suggested a role of FasL expressed on T cells in the iNSPCs apoptosis. Because nestin-positive iNSPCs were frequently observed in close association with endothelial cells[20,21] and $CD4^+$T cells (Supplementary Figure 3) in the poststroke brain, it is highly possible that activated T cells induce apoptosis of iNSPCs by cell to cell interactions.

To confirm this hypothesis *in vivo*, we administered T cells from the FasL-deficient (generalized lymphoproliferative disorder = spontaneous mutation in the Fas ligand gene; gld) mice,[25] stimulated by GITR–Ab, to poststroke SCID mice and analyzed the expression of nestin and Sox2 in the postischemic area by conventional RT-PCR. As gld-T cells stimulated by GITR–Ab showed enhanced GITR expression compared with non-stimulated gld-T cells similar to T cells from wild-type mice (Figure 8d; lanes 1 and 2, Figure 8f), the injected T cells were considered to be activated without

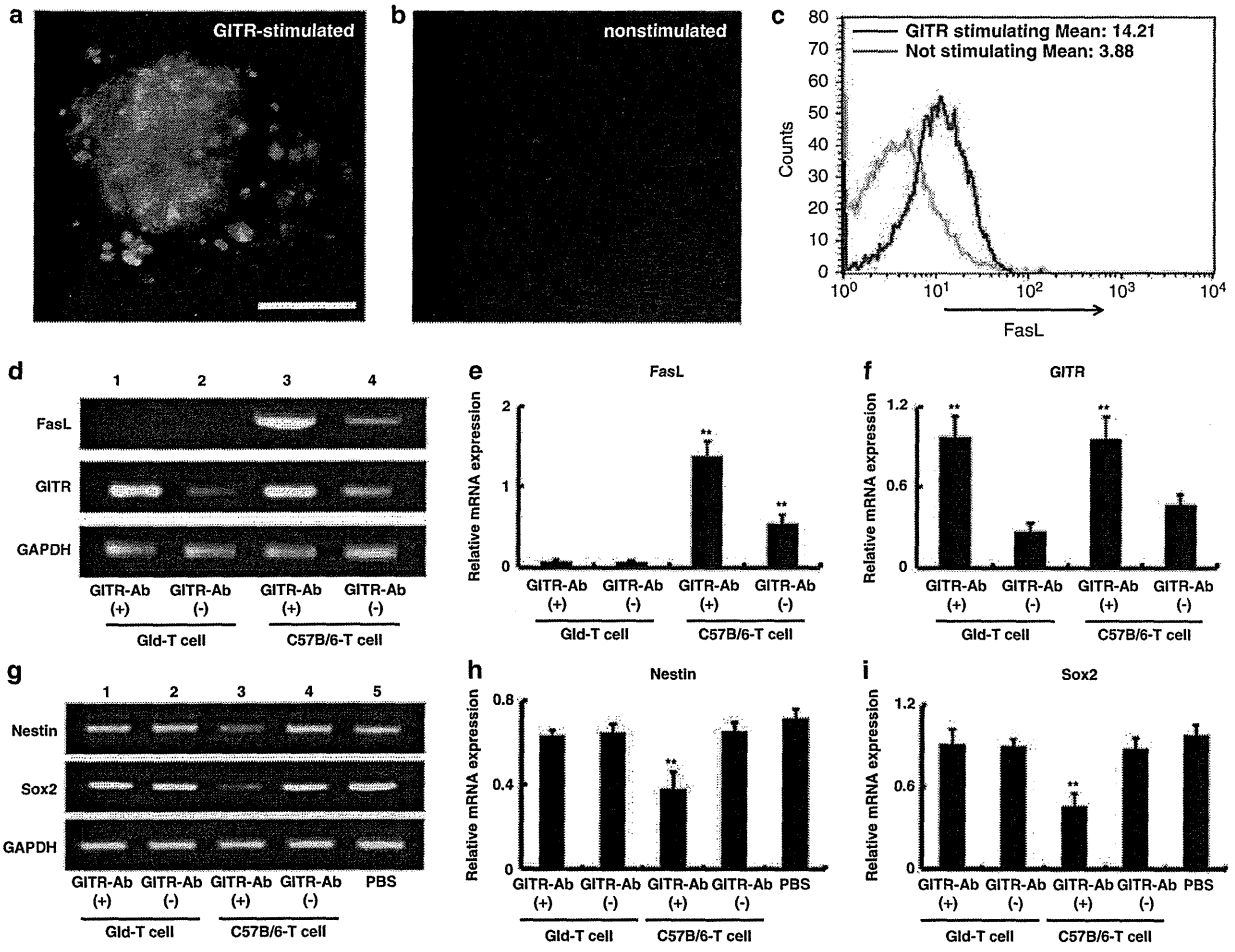

Figure 8 Involvement of Fas ligand expressed on the surface of T cells in survival/death of neural stem/progenitor cells. Incubation with GITR-stimulated T cells induced apoptotic cell death on neurospheres determined by Annexin V staining (**a**: green), whereas no cell death was observed in the presence of non-stimulated T cells (**b**). The upregulated FasL expressed on GITR-stimulated T cells was confirmed by FACS analysis (**c**: red line indicates the FasL expression on GITR-stimulated T cells, and green line on non-stimulated T cells in $CD4^+$ T cells). The mean channel values were displayed for FasL in the $CD4^+$ T cells. Conventional RT-PCR showed that T cells obtained from Gld mice (Gld-T cell) never expressed Fas ligand even after GITR stimulation (**d**: lanes 1 and 2; **e**), whereas T cells of wild C57/B6 mice expressed it (**d**: lanes 3 and 4; **e**). GITR stimulation upregulated GITR on T cells regardless of the presence of FasL (**d**: lanes 1 and 3; **f**). The group of GITR-stimulated T cells from C57B/6 only significantly upregulated FasL (**d** and **e**). (**a**) Scale bar: 100 μm. (**e** and **f**) $n=5$ for each experimental group. $^{**}P<0.01$ *versus* Gld-T cell groups or non-stimulated T (GITR–Ab(−)/C57B/6-T) cell group. Expression of nestin or Sox2 detected by conventional RT-PCR in the ischemic cortex of SCID mice 7 days after stroke was not affected by administration of Gld-T cells stimulated by GITR–Ab (**g**: first *versus* second lanes; **h** and **i**), although it was significantly decreased after treatment with wild-type (C57B/6) T cells stimulated by GITR-Ab (**g**: third *versus* fourth lanes; **h** and **i**). The relative expression of nestin or Sox2 was significantly suppressed only in the case of mice administered with FasL-expressed T cells stimulated by GITR–Ab. (**h** and **i**) $n=5$ for each experimental group. $^{**}P<0.01$ *versus* Gld-T cell groups, GITR(−)/C57B/6-T-cell group or PBS group. No significant difference was found among the other groups

expression of FasL (Figure 8e). Although administration of GITR-stimulated T cells from wild mice (C57/B6) significantly attenuated nestin and Sox2 expression (Figure 8g; lanes 3 and 4), administration of GITR-stimulated gld-T cells had no significant effect (Figure 8g; lanes 1 and 2). Relative expressions of nestin and Sox2 were attenuated only by GITR-stimulated wild-type T cells from wild mice, but not by GITR-stimulated gld-T cells or non-stimulated T cells (Figures 8h and i; $P<0.01$, among the five groups). These findings indicate that GITR-triggered activated $CD4^+$T cells directly induce Fas-mediated apoptosis of iNSPCs through possible cell to cell interactions.

Discussion

This study clearly demonstrated a key role of GITR triggering in regulation of neurogenesis after stroke, thereby delineating the contribution of activated T cells expressing GITR to the survival of neural stem/progenitor cells in the poststroke cortex. Because a subset of $CD4^+$T cells mainly expresses GITR after stroke, it is likely that activated $CD4^+$T cells triggered by GITR are harmful to the new-born cells. The current study also suggests possible mechanisms involving FasL- and TNF-α-induced cell death signals, suggesting interactions between iNSPCs and GITR-triggered T cells,

with the latter serving as negative regulators for CNS repair after cerebral infarction.

GITR was originally cloned from a glucocorticoid-treated hybridoma T-cell line as a TNF-receptor-like molecule induced by glucocorticoid-sensitive T cells.[12] GITR is now considered to be upregulated in T cells by T-cell receptor (TCR)-mediated activation.[26] As GITR-expressing T cells are resistant to glucocorticoid-induced cell death, it has been proposed that GITR, in conjunction with other TCR-induced factors, protects T cells from apoptosis.[26] In fact, GITR can be upregulated by viral infection[27] or acute lung inflammation.[15] In the present study, we have demonstrated for the first time that GITR is upregulated in T cells by ischemic insult to the brain, although previous reports have shown the role of GITR in ischemic damage on the kidney or the intestine.[28,29]

Consistent with our previous study,[8] $CD4^+$T cells predominantly migrated to the infarcted brain after stroke. The high number of $GITR^+CD4^+$T cells suggested that activated T-cell proliferation contributed to the poststroke inflammatory response. GITR has been reported to enhance the secretion of proinflammatory cytokines, such as IL-2 and IFN-γ, from $GITR^+$T cells.[30] In contrast, GITR triggering on $CD4^+CD25^+$Treg completely abrogates the suppressing effect of Treg,[13] which normally secrete anti-inflammatory cytokines such as IL-10.[31] Thus, we suggest that upregulation of the GITR expression in the brain can aggravate T-cell-mediated poststroke inflammation. The present study demonstrated that GITR triggering in poststroke mice enhanced, and its blocking ameliorated the poststroke inflammatory response as indicated by modulation of cytokines, such as IFN-γ, TNF-α and IL-10. These data suggest that T-cell-mediated poststroke inflammation can be modulated by the immune response deriving from GITR–GITRL interaction.

It is well known that cerebral injury induces a disturbance of the normally well-balanced interplay between the immune system and the CNS.[32] This process results in homeostatic signals being sent to various sites in the body through pathways of neuroimmunomodulation, including hypothalamic–pituitary–adrenal (HPA) axis. Activation of the HPA axis results in the production of glucocorticoid hormones. Although glucocorticoid does prevent inflammation by suppressing production of many proinflammatory mediators, including cytokines such as IL-1β and TNF-α, it also induces apoptosis in immature and mature T lymphocytes.[33] The latter may in turn lead to secondary immunodeficiency.[32] Alternatively, surviving T cells that are resistant to glucocorticoid stress express GITR and may contribute to the aggravation of inflammation.

Inflammation in neural tissue has long been suspected to have a role in stroke. Immune influence on adult neural stem cell regulation and function has also received much attention. Although the details of immune signaling in the CNS are not known, the impact of inflammatory signaling on adult neurogenesis is known to be focused on the activation of microglia as a source of proinflammatory cytokines, such as TNF-α, IL-6 and IL-1β. We and others[34] have proved that neural stem cells undergo apoptosis by TNF-α *in vitro*, suggesting that TNF-α has a negative effect on poststroke neurogenesis. Recent publication has revealed that GITR and GITRL are functionally expressed on brain microglia, and that the stimulation of GITRL can induce inflammatory activation of microglia.[35] However, as iNSPCs never expressed GITR, it is more likely that microglia contribute to iNSPC cell death indirectly via TNF-α, which is secreted from the activated microglia. We also propose that IFN-γ produced by activated $GITR^+$T cells stimulates microglia production of high levels of TNF-α to induce apoptosis of iNSPCs through TNFR-1. It also has been reported that TNF-related apoptosis-inducing ligand (TRAIL) has an important role in developing CNS injury, and that anti-TRAIL treatment prevents GITR expression induced by spinal cord injury.[36] As GITR-deficient mice showed attenuated TRAIL expression after SCI, blocking the GITR–GITRL interaction by GITR–Fc protein may protect from the inflammatory response via TRAIL-activated pathways.

In addition to cytokine effects on neurogenesis, we also proposed the Fas-mediated pathway that affects poststroke neurogenesis, as another target of immune signaling. Our previous study[8] had shown that Fas-positive iNSPCs underwent apoptosis in the poststroke cortex. The current study confirmed that $GITR^+$T cells expressing FasL triggered apoptosis of iNSPC *in vitro* and reduced the expression of nestin and Sox2 in the poststroke brain. These findings suggest that activated T cells act on Fas-expressing iNSPCs via cell to cell interactions in the poststroke brain, although it is very difficult to prove the functional contact between iNSPCs and Fas-expressing T cells *in vivo*. As nestin-positive iNSPCs are in close association with endothelial cells[20,21] where $CD4^+$T cells are infiltrated (Supplementary Figure 3), it is possible that activated T cells are in contact with neural stem/progenitor cells when the endothelial cells are damaged by ischemic insult. Although another system that activates neurogenesis through soluble FasL and Fas receptor in conventional neurogenic regions has been previously reported,[37] the current study may prove that the membrane-bound FasL expressed on T cells is essential for Fas-induced apoptosis.[38]

Recent study has proposed the contribution of Tregs in prevention of secondary infarct growth.[2,4] Because IL-10 signaling was mainly produced by $CD4^+CD25^+$Tregs and proinflammatory cytokines were downregulated in brains of IL-10 transgenic mice, Tregs apparently contribute to the anti-inflammatory system after stroke. Although $GITR^+$T cells are known to belong to Tregs, a recent study has emphasized that GITR is a marker for activated effector T cells.[39] The $CD4^+CD25^-$ T-cell-derived $GITR^+$ cells ($GITR^+$ non-Treg) are also known to activate self-reactive T cells by attenuating the function of Tregs,[13] indicating that they may harm the living cells by eliciting autoimmunity.[13,24] We demonstrated in the current study that blocking the GITR–GITRL interaction by GITR–Fc protein increased IL-10 expression in the poststroke cortex, suggesting that blocking such interactions enhanced Treg function as well as inhibition of effector T cell function. On the basis of these findings, the present study suggests that the novel therapies for stroke may ultimately include GITR-targeted manipulation of immune signaling.

Materials and Methods

All procedures were carried out under auspices of the Animal Care Committee of Hyogo College of Medicine, and were in accordance with the criteria outlined in the 'Guide for the Care and Use of Laboratory Animals' prepared by the National

Academy of Science. Quantitative analyses were conducted by investigators who were blinded to the experimental protocol and identity of the samples under study.

Induction of focal cerebral ischemia. Male, 5- to 7-week-old, CB17/Icr $^{+/+}$ Jcl mice (CB-17 mice; Clea Japan Inc., Tokyo, Japan) and CB-17/Icr$^{scid/scid}$ Jcl mice (SCID mice; CLEA Japan Inc.) were subjected to cerebral ischemia. Permanent focal cerebral ischemia was produced by ligation and disconnection of the distal portion of the left middle cerebral artery (MCA), as described in a previous study. In brief, the left MCA was isolated, electrocauterized and disconnected just distal to its crossing of the olfactory tract (distal M1 portion) under halothane inhalation. The infarcted area in mice of this background has been shown to be highly reproducible and limited to the ipsilateral cerebral cortex. Permanent MCA occlusion (MCO) is achieved by coagulating the vessel. In sham-operated mice, arteries were visualized but not coagulated.

Immunohistochemistry. To histochemically analyze the infarcted cortex, mice were deeply anesthetized with sodium pentobarbital and perfused transcardially with 4% paraformaldehyde. Brains were then removed, and coronal sections (14 μm) were stained with mouse antibodies against nestin (Millipore, Billerica, MA, USA; 1/100), Sox2 (Millipore; 1/100), NeuN (Millipore; 1/200), rabbit antibodies against caspase-3 active (R&D systems, Minneapolis, MN, USA; 1/100), CD3 (AnaSpec, San Jose, CA, USA; 1/100), CD31 (Santa Cruz Biotechnology, Santa Cruz, CA, USA; 1/100), rat antibody against CD4 (Biolegend, San Diego, CA, USA; 1/100) and GITR (eBioscience, San Diego, CA, USA; 1/100). As secondary antibodies, Alexa Fluor 488 or Alexa Fluor 555 goat anti-mouse, -rabbit or -rat IgG (Invitrogen, Carlsbad, CA, USA; 1/500) was used. Cell nuclei were stained with 4′, 6-diamino-2-phenylindole (DAPI, Kirkegaard & Perry Laboratories, Gaithersburg, MD, USA; 1/500). The number of nestin and Sox2 double-positive cells at the border of infarctions, including the infarcted and peri-infarcted areas (0.5 mm in width), was counted under a laser microscope (Olympus Corporation, Tokyo, Japan).

To perform quantitative analysis of T cells, all CD3–, CD4– or CD3–GITR-double-positive cells within the infarcted area were counted in the brain sections obtained from CB-17 mice at 3 h, 6 h, 24 h, 3 days and 7 days after stroke. Furthermore, active caspase-3 and nestin double-positive cells within the infarcted area were counted in the brain sections at 3 days after stroke. To investigate cell proliferation at 7 days after stroke, BrdU (Sigma-Aldrich Corporation, St. Louis, MO, USA; 50 mg/kg) was administered 6 h before fixation. Tissue was pretreated with 2N HCl for 30 min at 37°C and 0.1 M boric acid (pH 8.5) for 10 min at room temperature, and then stained with antibody against BrdU. Next, the number of positive cells for each marker was determined using modified Image J (National Institute of Mental Health, Bethesda, MD, USA) as per a previous report.[8] Results were expressed as the number of cells/mm^2.

The expression of Fas and TNFR-1 for neurosphere. To study the expression of Fas and TNFR-1in the neurosphere *in vitro*, immunochemistry was performed with rabbit antibody against Fas (Wako Pure Chemical Industries, Osaka, Japan; 1/100) or TNFR-1 (Santa Cruz Biotechnology; 1/100). As secondary antibodies, Alexa Fluor 488 or Alexa Fluor 555 goat anti-mouse IgG (Invitrogen; 1/500) was used. Cell nuclei were stained with DAPI (Kirkegaard & Perry Laboratories; 1/500).

Measurement of involution of the ipsilateral cerebral hemisphere volume. Thirty days after stroke, mice were perfused transcardially with 4% paraformaldehyde, brains were removed and coronal sections (14 μm) were stained with mouse antibodies against NeuN, followed by reaction with biotinylated goat anti-mouse IgG (Chemicon, Temecula, CA, USA; 1/500), ABC Elite reagent (Vector Laboratories, Burlingame, CA, USA) and DAB (Sigma-Aldrich Corporation) as chromogen. The area of the ipsilateral and contralateral cerebral hemisphere occupied by the neuronal markers, NeuN and MAP2, was calculated using Image J.[8] The ipsilateral and contralateral cerebral hemisphere volume was calculated by integrating the coronally oriented ipsilateral and contralateral cerebral hemisphere area as described previously.[8] Involution of the ipsilateral cerebral hemisphere volume was calculated as (ipsilateral/contralateral cerebral hemisphere volume).

FACS analysis of infiltrated lymphocytes into the ischemic brain. Animals were killed 1 or 7 days after MCO. The ischemic area of the brain was isolated. Tissues from the four operated mice were incubated with RPMI1640 (Invitrogen), containing 1 mg/ml collagenase (Wako Pure Chemical Industries) and 0.1 mg/ml DNAse I (Thermo Fisher Scientific, Waltham, MA, USA), and pressed through a 40-μm cell strainer[18] (BD Biosciences, Franklin Lakes, NJ, USA). The mononuclear cells were separated by Ficoll-paque plus (GE Healthcare, Piscataway, NJ, USA) centrifugation, and labeled with antibody cocktails (Per CP-CD3 (BD Biosciences), FITC-CD4 (eBioscience), PE-GITR (BD Biosciences) and APC-CD25 (eBioscience)). Rat IgG2a (eBioscience) was used as control isotype staining. The analysis of cells was performed by four-color flow cytometry on a FACSCalibur (BD Biosciences) using CELLQuest Software (BD Biosciences).

RNA isolation and PCR reaction. Total RNA was isolated from the cerebral cortex of the infarcted area using ISOGEN (Nippon gene, Tokyo, Japan), and was treated using Turbo DNA-free kit (Applied Biosystems, Foster city, CA, USA) in accordance with the manufacturer's protocol.

Quantity and quality of the isolated RNA was tested by using a Nanodrop 1000 (Thermo Fisher Scientific).

Quantitative real-time PCR was performed using TaqMan Gene Expression Assays and the ABI PRISM 7900HT Sequence Detection System (Applied Biosystems) with Real-time PCR Master Mix (Toyobo, Osaka, Japan). Three replicates were run for each sample in a 384-well format plate. TaqMan Gene Expression Assays IDs were described as follows. IFN-γ: Mm01168134_m1, TNF-γ: Mm00443258_m1, IL-10: Mm01288386_m1 and glyceraldehyde-3-phosphate dehydrogenase (GAPDH): Mm99999915_g1.

Conventional RT-PCR was performed using a PC-708 (Astec, Fukuoka, Japan) with Super Script III One step (Invitrogen). cDNA was amplified under the following conditions: 15 s at 94°C, 30 s at 60°C and 1 min at 68°C (35 cycles). PCR products were analyzed by electrophoresis using Mupid (Advance, Tokyo, Japan). The band intensity was determined with a LAS-1000 densitometer (Fuji Film, Tokyo, Japan). Primer sequences were as follows:

nestin, forward 5′-CACTAGAAAGCAGGAACCAG-3′ and reverse 5′-AGATGG TTCACAATCCTCTG-3′;
Sox2, forward 5′-TTGGGAGGGGTGCAAAAAGA-3′ and reverse 5′-CCTGCGA AGCGCCTAACGTA-3′;
GITR, forward 5′-CCACTGCCCACTGAGCAATAC-3′ and reverse 5′-GTAAAAC TGCGGTAAGTGAGGG-3′;
FasL, forward 5′-CTTGGGCTCCTCCAGGGTCAGT-3′ and reverse 5′-TCTCCT CCATTAGCACCAGATCC-3′; and
GAPDH, forward 5′-GGAAACCCAGAGGCATTGAC-3′ and reverse 5′-TCAGG ATCTGGCCCTTGAAC-3′.

For normalization of real-time data, GAPDH was used as an internal control.

Preparation of induced neural stem/progenitor cells. As described previously,[6] tissue from the ischemic cortex was mechanically dissociated by passage through 23- and 27-gauge needles to prepare a single-cell suspension. The resulting cell suspensions were incubated in a medium promoting formation of neurosphere-like clusters. Cells were incubated in tissue culture dishes (60 mm) with DMEM/F12 (Invitrogen) containing epidermal growth factor (EGF; Peprotech, Rocky Hill, NJ, USA; 20 ng/ml) and fibroblast growth factor-basic (FGF-2; Peprotech; 20 ng/ml). On day 7 after incubation, neurosphere-like cell clusters (primary spheres) were formed and were reseeded at a density of 10–15 neurospheres/well in 12-well low-binding plates.

Induction of apoptosis of neural stem/progenitor cells. To study the effect of TNF-α- or Fas-mediated signaling *in vitro*, neurospheres were incubated with TNF-α (R&D systems; 20 mg/ml and 100 mg/ml) or agonistic anti-Fas (Jo-2; BD Biosciences; 1 μg/ml) containing cycloheximide (CHZ; Sigma-Aldrich Corporation; 1 mg/ml),[40] agonistic anti-GITR (DTA-1; 10 μg/ml) or GITR–Fc fusion protein (6.25 μg/ml, Alexis Corporation, Lausen, Switzerland) in DMEM/F12 (Invitrogen) for 24 h. Next, the activity of caspase-3 was examined using a caspase-3 assay kit (Sigma-Aldrich Corporation) according to the manufacturer's protocol. Briefly, neurospheres were homogenized in lysis buffer and centrifuged at 20 000 *g* for 15 min. Supernatants were mixed with assay buffer and caspase-3 substrate. Absorbance at 405 nm was measured, and caspase-3 activity was calculated ($n = 3$, in each group) using a spectrophotometer (Beckman Coulter Inc., Brea, CA, USA). Caspase-3 activity was correlated with the protein concentration, which was determined by the DC protein assay (Lowry method; Bio-rad Laboratories Inc., Hercules, CA, USA). To confirm the cells undergoing apoptosis, neurospheres incubated with these reagents were stained with Annexin V (BD Biosciences), and were observed under a confocal laser scanning microscope (Carl Zeiss International, Jena, Germany).

To examine the apoptotic activity of T cells *in vitro*, T cells were obtained from the spleens of mice (several strains) involving CB-17 and gld (FasL deficient) and their C57/B6 backgrounds,[25] by using a nylon fiber column (Wako Pure Chemical Industries). T cells also were obtained from normal male C57BL/6 (Japan SLC, Shizuoka, Japan) or C57BL/6-Tg (CAG-EGFP) C14-Y01-FM131Osb transgenic mice (purchased from RIKEN BRC, Tsukuba, Japan). The T cells were stimulated with solid phase of anti-CD3ε antibody (BD Bioscience): T cells were incubated with GITR–Ab (DTA-1: 10 μg/ml) or control rat IgG (eBioscience) for 48 h in RPMI1640 (Invitrogen) in culture plate coated with 10 μg/ml of anti-CD3e antibody. Expression of FasL on GITR-stimulated T cells or non-stimulated T cells was analyzed with FACS. Each sample was labeled with antibody cocktails (PerCP-CD3, FITC-CD4 and PE-FasL (BD Biosciences)) The analysis of cells was performed by three-color flow cytometry on a FACSCalibur using CELLQuest Software. Then, 1×10^6 T cells were coincubated with neurospheres in DMEM/F12 (Invitrogen) for 24 h (10–15 neurospheres/well in 12-well low-binding plates). These neurospheres were stained with Annexin V and observed with a microscope, as mentioned above. GFP-Tg mice were purchased from CLEA Japan Inc.

Administration of GITR–Ab or GITR–Fc. GITR–Ab (100 μg/mice, DTA-1; eBioscience), GITR–Fc fusion protein (6.25 μg/mice)[16] or rat IgG isotype control (100 μg/mice, eBioscience) was intraperitoneally administered to mice at 3 h and 3 days after stroke.

Administration of T cells into poststroke SCID mice. T cells (1×10^6 cells/100 μl in PBS) obtained from several strains of mice (stimulated or non-stimulated by GITR-Ab), including CB-17, GFP-Tg, Gld- or C57/B6 mice, were injected intravenously into SCID mice at 48 h after stroke. Mice were subjected to histological examination after stroke. In another experiment, their brains were utilized for PCR analysis of nestin and Sox2.

Statistical analysis. Results were reported as the mean standard deviation. Statistical comparisons among groups were determined using one-way analysis of variance. Where indicated, individual comparisons were performed using Student's *t*-test. The groups with $P<0.01$ or, in some cases, $P<0.05$ differences were considered significant.

Conflict of Interest

The authors declare no conflict of interest.

Acknowledgements. This work was partially supported by a Grant-in-Aid for Scientific Research from the Ministry of Education, Culture, Sports, Science and Technology (21590473), and Hyogo Science and Technology Association. We thank Y Okinaka and Y Tanaka for technical assistance, and Dr. H Yamamoto for helpful discussion.

1. Hurn P, Subramanian S, Parker S, Afentoulis M, Kaler L, Vandenbark A *et al.* T- and B-cell-deficient mice with experimental stroke have reduced lesion size and inflammation. *J Cereb Blood Flow Metab* 2007; **27**: 1798–1805.
2. Liesz A, Suri-Payer E, Veltkamp C, Doerr H, Sommer C, Rivest S *et al.* Regulatory T cells are key cerebroprotective immunomodulators in acute experimental stroke. *Nat Med* 2009; **15**: 192–199.
3. Lambertsen K, Gregersen R, Meldgaard M, Clausen B, Heibøl E, Ladeby R *et al.* A role for interferon-gamma in focal cerebral ischemia in mice. *J Neuropathol Exp Neurol* 2004; **63**: 942–955.
4. de Bilbao F, Arsenijevic D, Moll T, Garcia-Gabay I, Vallet P, Langhans W *et al. In vivo* overexpression of interleukin-10 increases resistance to focal brain ischemia in mice. *J Neurochem* 2009; **110**: 12–22.
5. Arvidsson A, Collin T, Kirik D, Kokaia Z, Lindvall O. Neuronal replacement from endogenous precursors in the adult brain after stroke. *Nat Med* 2002; **8**: 963–970.
6. Nakagomi T, Taguchi A, Fujimori Y, Saino O, Nakano-Doi A, Kubo S *et al.* Isolation and characterization of neural stem/progenitor cells from post-stroke cerebral cortex in mice. *Eur J Neurosci* 2009; **29**: 1842–1852.
7. Taguchi A, Soma T, Tanaka H, Kanda T, Nishimura H, Yoshikawa H *et al.* Administration of CD34+ cells after stroke enhances neurogenesis via angiogenesis in a mouse model. *J Clin Invest* 2004; **114**: 330–338.
8. Saino O, Taguchi A, Nakagomi T, Nakano-Doi A, Kashiwamura S, Doe N *et al.* Immunodeficiency reduces neural stem/progenitor cell apoptosis and enhances neurogenesis in the cerebral cortex after stroke. *J Neurosci Res* 2010; **88**: 2385–2397.
9. Kleinschnitz C, Schwab N, Kraft P, Hagedorn I, Dreykluft A, Schwarz T *et al.* Early detrimental T-cell effects in experimental cerebral ischemia are neither related to adaptive immunity nor thrombus formation. *Blood* 2010; **115**: 3835–3842.
10. Yilmaz G, Arumugam T, Stokes K, Granger D. Role of T lymphocytes and interferon-gamma in ischemic stroke. *Circulation* 2006; **113**: 2105–2112.
11. Popovich PG, Longbrake EE. Can the immune system be harnessed to repair the CNS? *Nat Rev Neurosci* 2008; **9**: 481–493.
12. Nocentini G, Giunchi L, Ronchetti S, Krausz L, Bartoli A, Moraca R *et al.* A new member of the tumor necrosis factor/nerve growth factor receptor family inhibits T cell receptor-induced apoptosis. *Proc Natl Acad Sci USA* 1997; **94**: 6216–6221.
13. Shimizu J, Yamazaki S, Takahashi T, Ishida Y, Sakaguchi S. Stimulation of CD25(+)CD4(+) regulatory T cells through GITR breaks immunological self-tolerance. *Nat Immunol* 2002; **3**: 135–142.
14. Kwon B, Yu KY, Ni J, Yu GL, Jang IK, Kim YJ *et al.* Identification of a novel activation-inducible protein of the tumor necrosis factor receptor superfamily and its ligand. *J Biol Chem* 1999; **274**: 6056–6061.
15. Cuzzocrea S, Nocentini G, Di Paola R, Agostini M, Mazzon E, Ronchetti S *et al.* Proinflammatory role of glucocorticoid-induced TNF receptor-related gene in acute lung inflammation. *J Immunol* 2006; **177**: 631–641.
16. Nocentini G, Cuzzocrea S, Genovese T, Bianchini R, Mazzon E, Ronchetti S *et al.* Glucocorticoid-induced tumor necrosis factor receptor-related (GITR)-Fc fusion protein inhibits GITR triggering and protects from the inflammatory response after spinal cord injury. *Mol Pharmacol* 2008; **73**: 1610–1621.
17. Kohm A, Williams J, Miller S. Cutting edge: ligation of the glucocorticoid-induced TNF receptor enhances autoreactive CD4+ T cell activation and experimental autoimmune encephalomyelitis. *J Immunol* 2004; **172**: 4686–4690.
18. Gelderblom M, Leypoldt F, Steinbach K, Behrens D, Choe C, Siler D *et al.* Temporal and spatial dynamics of cerebral immune cell accumulation in stroke. *Stroke* 2009; **40**: 1849–1857.
19. Clausen BH, Lambertsen KL, Babcock AA, Holm TH, Dagnaes-Hansen F, Finsen B. Interleukin-1beta and tumor necrosis factor-alpha are expressed by different subsets of microglia and macrophages after ischemic stroke in mice. *J Neuroinflammation* 2008; **5**: 46.
20. Nakano-Doi A, Nakagomi T, Fujikawa M, Nakagomi N, Kubo S, Lu S *et al.* Bone Marrow mononuclear cells promote proliferation of endogenous neural stem cells through vascular niches after cerebral infarction. *Stem Cells* 2010; **28**: 1292–1302.
21. Nakagomi N, Nakagomi T, Kubo S, Nakano-Doi A, Saino O, Takata M *et al.* Endothelial cells support survival, proliferation, and neuronal differentiation of transplanted adult ischemia-induced neural stem/progenitor cells after cerebral infarction. *Stem Cells* 2009; **27**: 2185–2195.
22. Abematsu M, Tsujimura K, Yamano M, Saito M, Kohno K, Kohyama J *et al.* Neurons derived from transplanted neural stem cells restore disrupted neuronal circuitry in a mouse model of spinal cord injury. *J Clin Invest* 2010; **120**: 3255–3266.
23. Iosif R, Ekdahl C, Ahlenius H, Pronk C, Bonde S, Kokaia Z *et al.* Tumor necrosis factor receptor 1 is a negative regulator of progenitor proliferation in adult hippocampal neurogenesis. *J Neurosci* 2006; **26**: 9703–9712.
24. Muriglan SJ, Ramirez-Montagut T, Alpdogan O, Van Huystee TW, Eng JM, Hubbard VM *et al.* GITR activation induces an opposite effect on alloreactive CD4(+) and CD8(+) T cells in graft-versus-host disease. *J Exp Med* 2004; **200**: 149–157.
25. Schneider E, Moreau G, Arnould A, Vasseur F, Khodabaccus N, Dy M *et al.* Increased fetal and extramedullary hematopoiesis in Fas-deficient C57BL/6-lpr/lpr mice. *Blood* 1999; **94**: 2613–2621.
26. Zhan Y, Funda DP, Every AL, Fundova P, Purton JF, Liddicoat DR *et al.* TCR-mediated activation promotes GITR upregulation in T cells and resistance to glucocorticoid-induced death. *Int Immunol* 2004; **16**: 1315–1321.
27. Suvas S, Kim B, Sarangi PP, Tone M, Waldmann H, Rouse BT. *In vivo* kinetics of GITR and GITR ligand expression and their functional significance in regulating viral immunopathology. *J Virol* 2005; **79**: 11935–11942.
28. Monteiro RM, Camara NO, Rodrigues MM, Tzelepis F, Damião MJ, Cenedeze MA *et al.* A role for regulatory T cells in renal acute kidney injury. *Transpl Immunol* 2009; **21**: 50–55.
29. Cuzzocrea S, Nocentini G, Di Paola R, Mazzon E, Ronchetti S, Genovese T *et al.* Glucocorticoid-induced TNF receptor family gene (GITR) knockout mice exhibit a resistance to splanchnic artery occlusion (SAO) shock. *J Leukoc Biol* 2004; **76**: 933–940.
30. Ronchetti S, Zollo O, Bruscoli S, Agostini M, Bianchini R, Nocentini G *et al.* GITR, a member of the TNF receptor superfamily, is costimulatory to mouse T lymphocyte subpopulations. *Eur J Immunol* 2004; **34**: 613–622.
31. O'Garra A, Vieira P. Regulatory T cells and mechanisms of immune system control. *Nat Med* 2004; **10**: 801–805.
32. Meisel C, Schwab JM, Prass K, Meisel A, Dirnagl U. Central nervous system injury-induced immune deficiency syndrome. *Nat Rev Neurosci* 2005; **6**: 775–786.
33. Zacharchuk CM, Meræep M, Chakraborti PK, Simons SS, Ashwell JD. Programmed T lymphocyte death. Cell activation- and steroid-induced pathways are mutually antagonistic. *J Immunol* 1990; **145**: 4037–4045.
34. Iosif R, Ahlenius H, Ekdahl C, Darsalia V, Thored P, Jovinge S *et al.* Suppression of stroke-induced progenitor proliferation in adult subventricular zone by tumor necrosis factor receptor 1. *J Cereb Blood Flow Metab* 2008; **28**: 1574–1587.
35. Hwang H, Lee S, Lee W, Lee H, Suk K. Stimulation of glucocorticoid-induced tumor necrosis factor receptor family-related protein ligand (GITRL) induces inflammatory activation of microglia in culture. *J Neurosci Res* 2010; **88**: 2188–2196.

36. Cantarella G, Di Benedetto G, Scollo M, Paterniti I, Cuzzocrea S, Bosco P *et al.* Neutralization of tumor necrosis factor-related apoptosis-inducing ligand reduces spinal cord injury damage in mice. *Neuropsychopharmacology* 2010; **35**: 1302–1314.
37. Corsini NS, Sancho-Martinez I, Laudenklos S, Glagow D, Kumar S, Letellier E *et al.* The death receptor CD95 activates adult neural stem cells for working memory formation and brain repair. *Cell Stem Cell* 2009; **5**: 178–190.
38. O' Reilly LA, Tai L, Lee L, Kruse EA, Grabow S, Fairlie WD *et al.* Membrane-bound Fas ligand only is essential for Fas-induced apoptosis. *Nature* 2009; **461**: 659–663.
39. Nocentini G, Ronchetti S, Cuzzocrea S, Riccardi C. GITR/GITRL: more than an effector T cell co-stimulatory system. *Eur J Immunol* 2007; **37**: 1165–1169.
40. Nishimura Y, Hirabayashi Y, Matsuzaki Y, Musette P, Ishii A, Nakauchi H *et al. In vivo* analysis of Fas antigen-mediated apoptosis: effects of agonistic anti-mouse Fas mAb on thymus, spleen and liver. *Int Immunol* 1997; **9**: 307–316.

Supplementary Information accompanies the paper on Cell Death and Differentiation website (http://www.nature.com/cdd)

Experimental Neurology 233 (2012) 481–489

Contents lists available at SciVerse ScienceDirect

Experimental Neurology

journal homepage: www.elsevier.com/locate/yexnr

Cerebral blood flow during reperfusion predicts later brain damage in a mouse and a rat model of neonatal hypoxic–ischemic encephalopathy

Makiko Ohshima [a], Masahiro Tsuji [a,*], Akihiko Taguchi [a], Yukiko Kasahara [a], Tomoaki Ikeda [a,b]

[a] Department of Regenerative Medicine and Tissue Engineering, National Cerebral and Cardiovascular Center Research Institute, 5-7-1, Fujishiro-dai, Suita, Osaka, 565-8565, Japan
[b] Department of Perinatology, National Cerebral and Cardiovascular Center Research Institute, 5-7-1, Fujishiro-dai, Suita, Osaka, 565-8565, Japan

ARTICLE INFO

Article history:
Received 12 September 2011
Accepted 11 November 2011
Available online 27 November 2011

Keywords:
Hypoxic–ischemic brain injury
Cerebral blood flow
Reperfusion
Laser speckle flowmetry
Neonatal
Rat
Mouse
Dexamethasone

ABSTRACT

Children with severe neonatal hypoxic–ischemic encephalopathy (HIE) die or develop life-long neurological impairments such as cerebral palsy and mental retardation. Decreased regional cerebral blood flow (CBF) is believed to be the predominant factor that determines the level of tissue injury in the immature brain. However, the spatio-temporal profiles of CBF after neonatal HIE are not well understood. CB17 mouse and Wistar rat pups were exposed to a unilateral hypoxic–ischemic (HI) insult at eight or seven days of age. Laser speckle imaging sequentially measured the cortical surface CBF before the hypoxic exposure and until 24 h after the hypoxic exposure. Seven days after the HI insult, brain damage was morphologically assessed by measuring the hemispheric volumes and by semi-quantitative scoring for neuropathologic injury. The mean CBF on the ipsilateral hemisphere in mice decreased after carotid artery ligation. After the end of hypoxic insult (i.e., the reperfusion phase), the mean CBF level gradually rose and nearly attained its pre-surgery level by 9 h of reperfusion. It then decreased. The degree of reduced CBF during reperfusion was well correlated with the degree of later morphological brain damage. The correlation was the strongest when the CBF was measured in the ischemic core region at 24 h of reperfusion in mice ($R^2 = 0.89$). A similar trend in results was found in rats. These results suggest that the CBF level during reperfusion may be a useful predictive factor for later brain damage in immature mice. This may enable optimizing brain damage for detail analyses.

Introduction

Children with severe neonatal hypoxic–ischemic encephalopathy (HIE) typically die or develop life-long neurological impairments such as cerebral palsy, mental retardation, and epilepsy (van Handel et al., 2007). No therapeutic method is available for perinatal HIE, apart from initiating hypothermia within 6 h after birth. An important issue in neonatal practice is the early detection of pathophysiological factors that are associated with permanent brain damage. Extensive laboratory research with experimental models is being performed to understand the mechanisms of brain injury and to find neuroprotective therapies. The Rice–Vannucci model, which combines permanent unilateral ligation of a carotid artery with exposure to hypoxia for 2 to 3 h in seven-day-old rat pups, has been widely used to study the physiological and therapeutic variables of neonatal hypoxic–ischemic (HI) injury (Johnston et al., 2005; Rice et al., 1981). This model has also been adapted for use in neonatal mice.

Decreased regional cerebral blood flow (CBF) is the predominant factor that determines the topography of tissue injury in the immature rodent brain, although metabolic factors (i.e., intrinsic vulnerability) may influence injury in some brain structures (Ringel et al., 1991; Vannucci et al., 1988). In immature rats with an HI injury, radioactive tracers in coronal sections show a residual columnar perfusion deficit within the cerebral cortex, which corresponds closely to the pathological pattern of injury within this structure. The pathological pattern of injury is characterized by alternating columns of normal and damaged neurons, which are oriented at a right angle to the pial surface. CBF is rarely monitored during and after HI insult in immature rodent models, mainly because of the technical difficulties and invasiveness involved in measuring it. Therefore, little is known about the spatial and temporal extent of CBF response during the reperfusion period after an HI insult.

The autoradiographic techniques for analyzing CBF in small animals entail sacrificing the animals at the time of measurement. A less invasive method, laser Doppler flowmetry (LDF), has been widely used to monitor relative perfusion changes. The LDF technique uses a single-point measurement in which the hemodynamics of an area covering 1 mm^3 to 2 mm^3 can be measured from the tip of a probe (Stern et al., 1977). CBF measured at a small arbitrarily selected area may not accurately reflect the hemodynamics of the cerebral hemisphere, and the

Abbreviations: NHIE, neonatal hypoxic–ischemic encephalopathy; HI, hypoxic–ischemic, hypoxia–ischemia; CBF, cerebral blood flow; LSF, laser speckle flowmetry; LDF, laser Doppler flowmetry; ROI, region of interest; MCA, middle cerebral artery; MRI, magnetic resonance imaging; DWI, Diffusion-weighted MRI; ANOVA, analysis of variance.

* Corresponding author. Fax: +81 6 6835 5496.
E-mail addresses: oshimam@ri.ncvc.go.jp, mtsujimd@ybb.ne.jp (M. Ohshima), mtsuji@ri.ncvc.go.jp (M. Tsuji), taguchi@ri.ncvc.go.jp (A. Taguchi), kasahara@ri.ncvc.go.jp (Y. Kasahara), tikeda@hsp.ncvc.go.jp (T. Ikeda).

0014-4886/$ – see front matter © 2011 Elsevier Inc. All rights reserved.
doi:10.1016/j.expneurol.2011.11.025

probe-position-specific manner of measurement makes repeated intermittent measurements unreliable. Since LDF generally requires the attachment of a probe onto the skull or the dura, long-term observation would excessively strain the pups. Hence, the monitoring duration with LDF in most cases is short, being less than 1 (Liu et al., 1999; Matsiukevich, et al., 2010; Taniguchi et al., 2007), or 2 h after the end of hypoxic exposure (Fabian et al., 2008; Ioroi et al., 1998). To our knowledge, there is only one report in which the CBF was observed beyond the early perfusion phase in a rodent model of neonatal HIE (Wainwright et al., 2007). Laser Doppler perfusion imaging is a recent development in LDF that extends its power to the two-dimensional measurement of tissue perfusion. However, laser Doppler perfusion imaging cannot be used to dynamically image high frequency blood-flow fluctuations since the temporal separation between the first and last image points within a scan can be several minutes. In addition, its resolution is not very high, ranging from 100 μm/pixel to 1.0 mm/pixel (Forrester et al., 2002; Riyamongkol et al., 2002).

The laser speckle method for imaging vascular structure in a tissue has been available since the 1980s. It has recently been revised to measure CBF, as first described by Dunn et al. (2001). For a duration of several milliseconds to several hours, the speckle imaging method is able to accurately image the cortical blood-flow response over an area ranging from a few millimeters to the whole rodent brain (Dunn et al., 2001). Laser speckle flowmetry (LSF) provides excellent spatial resolution, even through an intact skull. This allows the measurement of CBF changes occurring within the pial vasculature (Ayata et al., 2004). The laser speckle technique primarily measures the velocity of scattering particles (e.g., red blood cells). LSF provides an index of perfusion that has a linear relationship with the absolute CBF value (which is measured by the [^{14}C]iodoamphetamine technique (Ayata et al., 2004) and by the clearance rate of umbelliferone (Strong et al., 2006)). LSF enables the long-term observation of CBF (Fujita et al., 2010). To our knowledge, the use of two-dimensional laser speckle perfusion imaging to observe CBF has never been investigated in immature rodent models of HI insult or stroke.

There is significant inter- and intra-litter variability in the extent of the brain injury in the HI model: a subset of pups suffers no perceivable brain injury, while other pups suffer massive hemispheric infarct (Sheldon et al., 1998). This also holds true in neonatal stroke models (Bonnin et al., 2011; Comi, et al., 2005; Wendland et al., 2008). The variability in animal models resembles the variability seen in human infants with neonatal HIE. In a population-based study, the teenage outcome of children who had been born with moderate neonatal HIE was quite variable: 35% had cerebral palsy or other major neuroimpairments; 46% had cognitive problems without cerebral palsy; and 9% had no problems (Lindström et al., 2006). Hence, it is no wonder that some pups may have no lesion after an HI insult. The variability in animal models, however, makes detailed preclinical analyses difficult to perform. Efforts have been made to offset this hindrance and, in particular, to exclude subjects with no lesion, but there is no widely used method to optimize degree of brain injury. A few laboratories use parameters—such as apparent diffusion coefficient (ADC) obtained by magnetic resonance imaging (MRI) (Derugin et al., 2000; Wendland et al., 2008), or the CBF obtained by color-coded pulsed Doppler ultrasound imaging (Bonnin et al., 2011)—to exclude pups without a lesion at an early stage of brain injury. The objectives of our study are: 1) to show temporal changes in CBF in a mouse model and in a rat model of neonatal HIE and 2) to examine the correlation between CBF during the early stage of HI injury and later morphological brain damage.

Materials and methods

Hypoxia–ischemia procedure

All experiments were performed in accordance with protocols approved by the Experimental Animal Care and Use Committee of the National Cerebral and Cardiovascular Center. Eight-day-old (postnatal day 8, [P8]) male and female CB17 mouse pups (CLEA Japan Inc., Tokyo, Japan) and seven-day-old (P7) male and female Wistar rat pups (Japan SLC Inc., Hamamatsu, Japan) were prepared for surgery. Under isoflurane anesthesia (4.0% for induction and 1.5% to 2.0% for maintenance), the left carotid artery was permanently occluded in the mouse and rat pups. After a one- to two-hour recovery period, the mouse pups were subjected to hypoxia (8% oxygen and 92% nitrogen, at 33.0 °C) for 30 min and the rat pups were subjected to hypoxia for 120 min. After a 60-min recovery period in a temperature-controlled incubator, the pups were returned to their dams and kept in a standard environment.

Laser speckle blood-flow imaging

In 23 mice and 33 rats, the cortical surface CBF was sequentially measured by a laser speckle flowmetry (LSF) imaging system (Omegazone, Omegawave Inc., Tokyo, Japan) at several time points: pre-surgery; pre-hypoxia (which is post-surgery); and 0 h, 1 h, 2.5 h, 6 h, 9 h, and 24 h after the end of hypoxia (i.e. after the start of reperfusion). The theory and technique for LSF have been described in detail elsewhere (Dunn et al., 2001; Forrester et al., 2002). In brief, the animals were placed in a prone position and spontaneously breathed under isoflurane anesthesia. The animal's skull was exposed by a midline scalp incision and the skull surface was diffusely illuminated by a 780 nm laser light. The penetration depth of the laser is approximately 500 μm. The scattered light was filtered and detected by a charge coupled device (CCD) camera positioned above the animal's head. Raw speckle images were used to compute the speckle contrast, which is a measure of speckle visibility that is related to the number and velocity of moving particles (in this case, CBF). Color-coded blood-flow images were obtained in the high-resolution mode (638 pixels × 480 pixels; 1 image/s). Five consecutive raw speckle images were acquired at 1 Hz, and then averaged. For analytical accuracy in repositioning of the animal's head and regions of interest (ROIs) between imagings, we set the size and the position of an ROI, based on a line drawn from the bregma to the lambda (Fig. 1A). We measured the CBF in three ROIs: the Core (the ischemic core region of the middle cerebral artery (MCA) territory); the Penumbra (the penumbra region of the MCA territory by the sagittal suture); and the MCA region (the broader region covering most of the MCA territory, including the Core and the Penumbra) (Fig. 1A). The same grid was used to set the three matching regions on the contralateral side. The total measuring procedure took approximately 3 min per pup.

Quantitative histological analysis

Seven days after the HI insult, the animals were deeply anesthetized with an overdose of pentobarbital and intracardially perfusion-fixed with 4% paraformaldehyde. After the perfusion, an animal's brain was removed and coronally sectioned in slices 2-mm thick by using a rat brain slicer (Neuroscience Inc., Tokyo, Japan). The area (in mm^2) of the contralateral and ipsilateral hemispheres in each brain section was measured, using NIH Image software (ImageJ, 1.43r, NIH, Bethesda, USA). The hemispheric volume of the brain of each pup was estimated by summing the hemispheric area of the brain slices and multiplying the sum by the section interval thickness. The injury was evaluated by using hematoxylin–eosin-stained sections from four brain regions: the cortex, striatum, hippocampus, and thalamus. We used the system we previously developed for evaluating neuropathologic injury in the present study (Tsuji et al., 2004). Neuropathologic injury in the cerebral cortex was scored on a scale ranging from 0 to 4 points (0, no injury; 4, extensive confluent infarction). Neuropathologic injury in the hippocampus, striatum, and thalamus was scored on a scale ranging from 0 to 6 points. The total score (ranging from 0 to 22 points) was the sum of these ratings. The

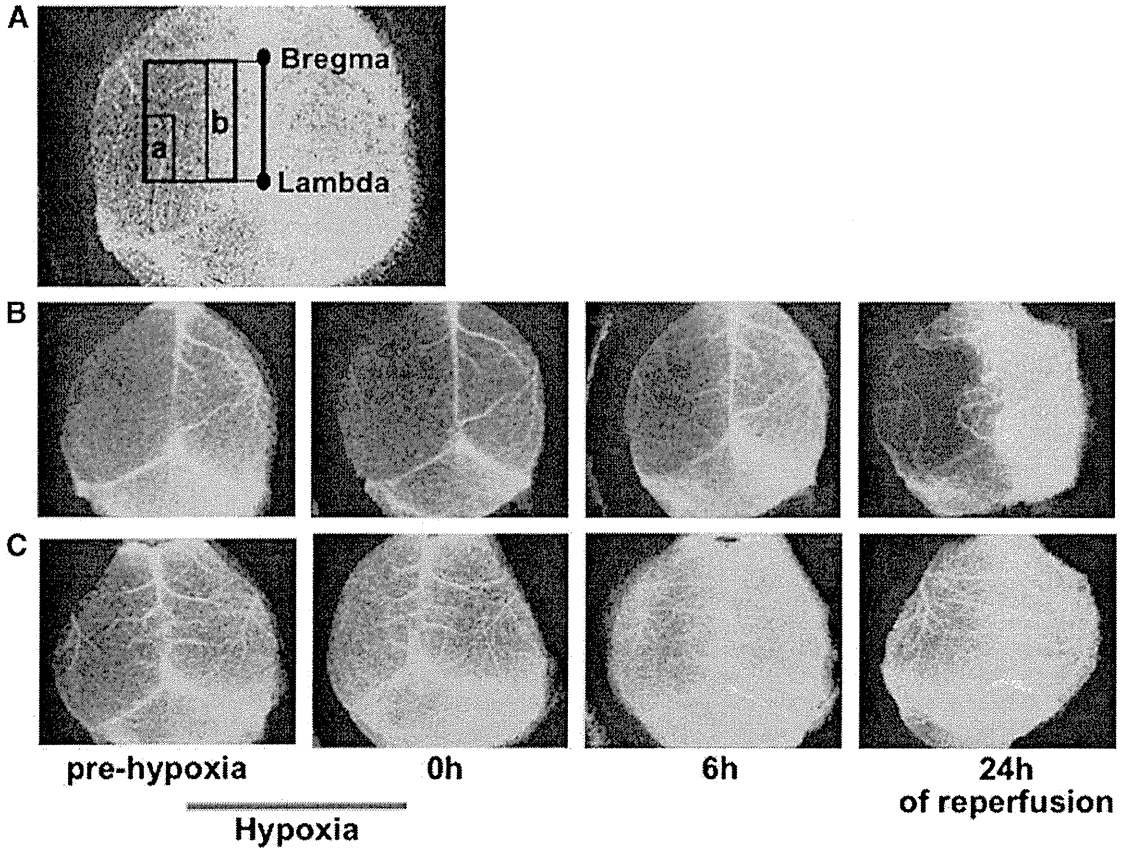

Fig. 1. We measured the cerebral blood flow (CBF) in three regions of interest (ROIs) (A): the Core (the ischemic core region of the middle cerebral artery [MCA] territory) (a); the Penumbra (the penumbra region of the MCA territory by the sagittal suture (b); and the MCA region (a broad region covering most of the MCA territory including the Core and the Penumbra) (represented by a square with bold lines). We set the grid to standardize the size and position of the ROIs. A line is drawn from the bregma to the lambda. Using this line, a square is drawn. The line perpendicular to the bregma–lambda line is divided into four equal segments, establishing four quarter-rectangles. The second quarter-rectangle from the center (b) is the Penumbra. The posterior half of the most lateral quarter-rectangle (a) is the Core. The whole square, excluding the most medial quarter-rectangle, is the MCA region. Representative laser speckle images were sequentially taken at several time points in two mouse pups. One pup (B) shows progressive reduction of CBF on the ipsilateral hemisphere of the carotid artery ligation, while the other pup (C) shows restoration of CBF.

hemispheric volume measurement and neuropathological scoring were assessed blindly.

Drug administration

In a different cohort, we used dexamethasone to examine how drug treatment affects the correlation between CBF and brain damage. Dexamethasone is a known neuroprotective drug, if it is administered before a neurologic insult in rodents (Tuor, 1995). On postnatal day 7, mouse littermates were randomly assigned to either a dexamethasone-treated group (n = 17) or a vehicle-treated group (n = 16). In the former group, 0.5 mg/kg of dexamethasone dissolved in normal saline (40 μl) was injected intraperitoneally 24 h before the HI insult. The vehicle was administered in the same manner.

Statistics

Hemispheric differences in CBF were assessed using repeated-measures two-way analysis of variance (ANOVA), followed by the Bonferroni–Dunn test. The temporal changes in CBF were analyzed by the Friedman test, followed by the Bonferroni–Dunn test. Pearson's productmoment correlation coefficient analysis was performed to determine the correlation between CBF and brain injury. Linear regression analysis and the Student *t*-test were performed to assess the effects of dexamethasone. Differences were considered significant at $P<0.05$. The results are presented as the mean ± standard error of the mean (SEM).

Results

Temporal profile of CBF in mice

LSF imaging through the intact mouse skull demonstrated clear two-dimensional images of the cortical surface blood flow (Figs. 1B, C). The surface blood flow during the pre-hypoxia period (i.e., after carotid artery occlusion but immediately before hypoxic exposure) decreased in the MCA territory on the ipsilateral side of the carotid artery occlusion in all mouse pups. In some pups, the CBF on the ipsilateral side of the carotid artery occlusion remained decreased or decreased further during the reperfusion phase (Fig. 1B). In other pups, the CBF on the ipsilateral side was nearly restored to the same level as on the contralateral side (Fig. 1C).

On the ipsilateral side of the carotid artery occlusion, temporal profiles of the mean surface CBF in the Core and the MCA region (but not the Penumbra region) differed significantly from the matching regions on the contralateral side, based on repeated-measures two-way ANOVA (Figs. 2A–C). The mean surface CBF in each of the three regions of each hemisphere was significantly decreased before the hypoxic exposure, compared with mean surface CBF in these regions before surgery. During the early reperfusion phase, the mean

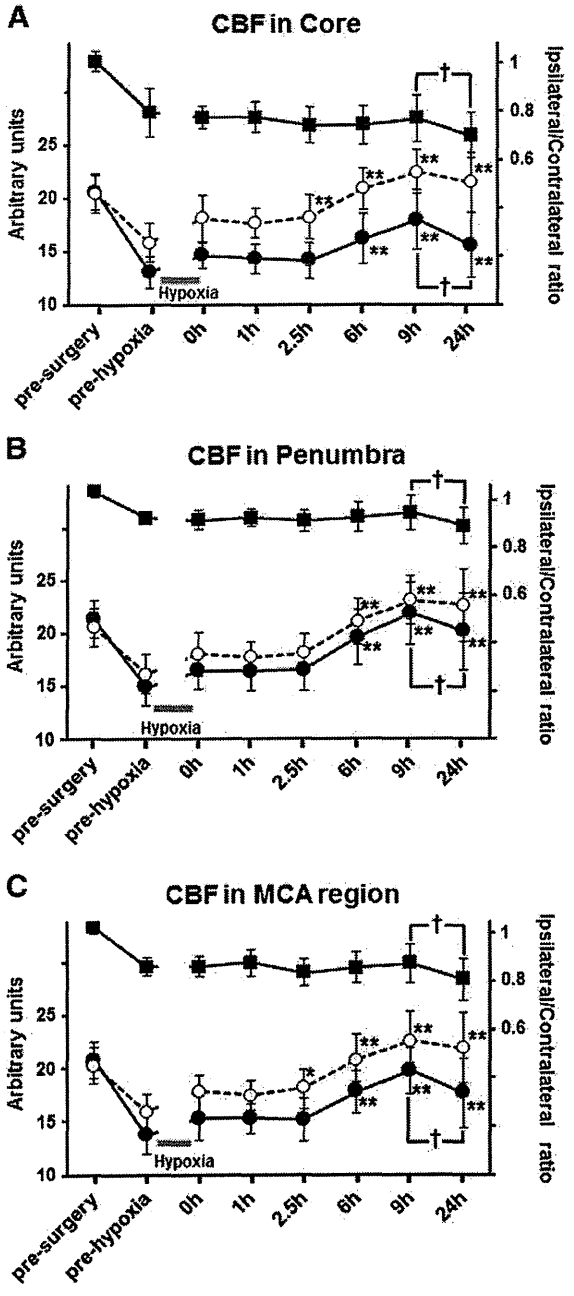

Fig. 2. The temporal profile of the mean CBF in mice in (A) the Core region; (B) the Penumbra region; and (C) the MCA region. The line with closed circles represents the ipsilateral CBF; the dashed line with open circles represents the contralateral CBF; the line with closed squares represents the ipsilateral/contralateral CBF ratio. The surface CBF level in each ROI in each hemisphere is significantly increased 6 h, 9 h, and 24 h after the end of hypoxia (i.e. the reperfusion phase), compared with the pre-hypoxia CBF level. *$p<0.05$; **$p<0.01$. The CBF in each ROI in the ipsilateral hemisphere (but not the contralateral hemisphere) is significantly decreased at 24 h, compared with the CBF at 9 h. † $p<0.05$

CBF in all three regions of both hemispheres increased slightly from the pre-hypoxic level; however, the increases were not statistically significant. During the late reperfusion phase (i.e., 6 h, 9 h, and 24 h after the end of hypoxia), the mean CBF in the three regions of both hemispheres increased significantly, compared with the mean CBF before the hypoxia. After 9 h of reperfusion, the mean CBF in the Penumbra region in the ipsilateral hemisphere and in all regions in the contralateral hemisphere were restored to their pre-surgery levels. At 24 h, the mean CBF in the three regions in the contralateral hemisphere remained the same; however, the mean CBF in all the three regions in the ipsilateral hemisphere was significantly decreased after 9 h. In the three regions, the ratio of the ipsilateral CBF to the contralateral CBF did not change significantly from before the hypoxic exposure to 9 h after the hypoxic exposure. From 9 h to 24 h, the ratio decreased significantly in the three regions.

Correlation between the CBF and later brain injury in mice

Brain injury was assessed histologically seven days after the HI insult. The CBF in each region at each time point was then compared with the histological brain injury in the mice. This was to determine whether the surface CBF (as measured by LSF during the reperfusion phase) can be used as an early indicator of later histological injury after an HI insult. The ratio of the ipsilateral CBF to the contralateral CBF was compared with the ratio of the ipsilateral hemispheric volume to the contralateral hemispheric volume (Fig. 3). Linear regression analysis demonstrated that the longer the time after the hypoxic exposure, the stronger was the correlation between the degree of reduced CBF and the degree of brain damage. The correlation was stronger in the Core than in the other two regions. Of all the regions and time points measured, the CBF in the Core at 24 h of reperfusion had the strongest correlation with brain injury ($R^2=0.89$).

We also used neuropathological injury scoring to examine the correlation between CBF and brain injury. Linear regression analysis demonstrated that the surface CBF in the Core at 24 h was significantly correlated with neuropathological scores in all four anatomical structures (the hippocampus, thalamus, cortex, and striatum) that were examined seven days after the HI insult (Fig. 4). Interestingly, the correlation was strongest for the injury score in the hippocampus ($R^2=0.58$) (data not shown), followed by the injury score in the thalamus. The correlation for the injury score in the cortex ($R^2=0.36$) was weaker than that of total score ($R^2=0.51$).

The effect of drug treatment on the correlation between CBF and later brain injury

The hemispheric volume was assessed seven days after the HI insult. Dexamethasone pretreatment, as expected, significantly reduced brain injury. However, this treatment did not improve CBF 24 h after the HI insult. The correlation between the CBF and brain injury in the dexamethasone-treated group was not significant ($P=0.08$) (Fig. 5). The loss of correlation between the CBF and brain injury after dexamethasone treatment indicates that its neuroprotective mechanisms are independent of CBF, at least at the time of measurement.

Temporal profile of CBF and its correlation with later brain injury in rats

Based on the results of repeated-measures two-way ANOVA, the temporal profile of the mean surface CBF in the Core on the ipsilateral side of the carotid artery occlusion significantly differed from the matching regions on the contralateral side in rats (Fig. 6A). The mean surface CBF in the Core on the ipsilateral hemisphere before the hypoxic exposure was significantly decreased from its pre-surgery level, while the mean surface CBF in the Core on the contralateral hemisphere remained the same. The mean CBF in the Core in both hemispheres significantly increased after 2.5 h of reperfusion, compared with the mean CBF before hypoxia. After 6 h of reperfusion, the mean CBF in the Core on the ipsilateral side was restored to its pre-surgery level, and the mean CBF in the matching region on the contralateral side increased beyond its pre-surgery level. The mean CBF in the Core of each hemisphere at 24 h was significantly decreased from its level at the previous time point measurement. The

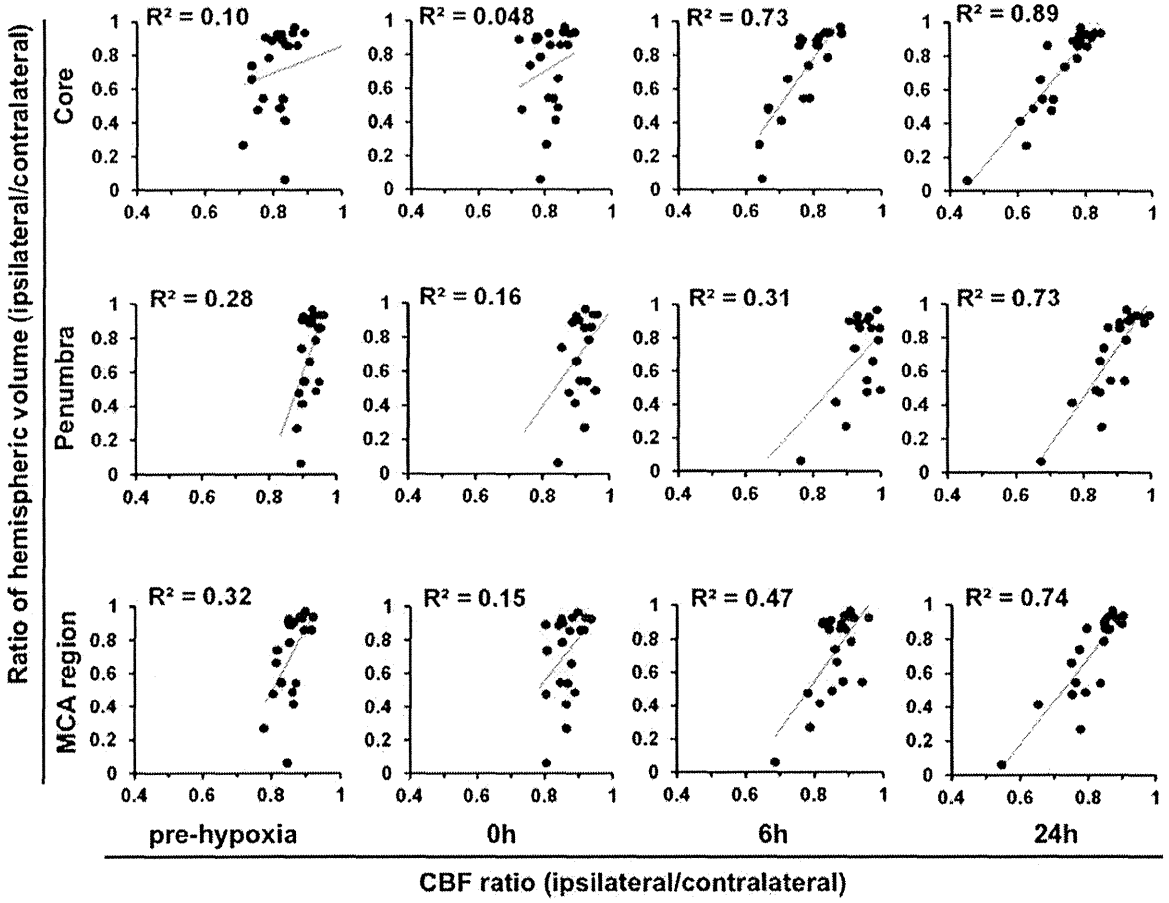

Fig. 3. The ratio of the ipsilateral CBF to the contralateral CBF at each time point was compared with the ratio of the ipsilateral hemispheric volume to the contralateral hemispheric volume (which was assessed seven days after the HI insult in the mice). The correlation between the degree of CBF reduction and the degree of brain damage is stronger in the Core than in the other two regions. The correlation was stronger at the later time points. Of all the time points and regions measured, the CBF in the Core at 24 h of reperfusion has the strongest correlation with later brain injury ($R^2 = 0.89$).

ratio of the ipsilateral CBF to the contralateral CBF increased from 2.5 h of reperfusion onward, compared with the pre-hypoxia ratio.

Among the three regions, the correlation between CBF and later brain injury (as assessed by the hemispheric volume) was the strongest in the Core in rats. This was also the case in mice. In the Core region, the CBF at 6 h of reperfusion had the strongest correlation with later brain injury ($R^2 = 0.35$) (Fig. 6B). When assessed by neuropathological injury scoring, a correlation was evident between the CBF and brain injury. Linear regression analysis demonstrated that the CBF in the Core at 6 h was significantly correlated with the total neuropathological scores, which were assessed seven days after the HI insult ($R^2 = 0.27$) (data not shown). These correlations were weaker in rats than in mice.

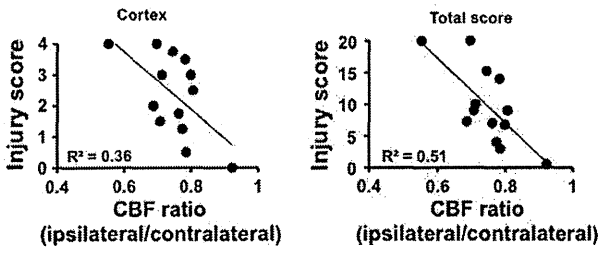

Fig. 4. The ratio of the ipsilateral CBF to contralateral CBF 24 h after the HI insult was compared with brain injury (as assessed by neuropathological scoring seven days after the HI exposure). Linear regression analysis demonstrates that the surface CBF in the Core at 24 h is significantly correlated with the neuropathological scores in the cortex and with the total score (which combines the scores of the cortex, hippocampus, striatum, and thalamus).

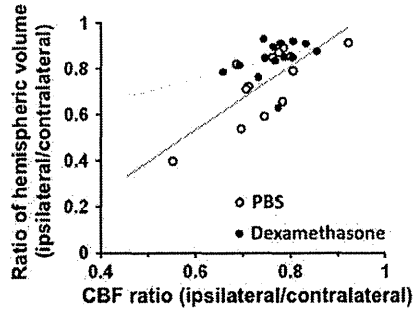

Fig. 5. The hemispheric volume (measured seven days after the HI insult) was used to assess the effect of the neuroprotective drug dexamethasone on the correlation between CBF (24 h after the HI insult) and brain injury. The data points show the correlation between CBF and brain injury in the PBS-pretreated mice and the dexamethasone-pretreated mice. The data points for the dexamethasone-pretreated mice tends to be shifted toward the top of the graph (indicating less brain injury), but is not shifted in the horizontal axis (indicating no change in the CBF).

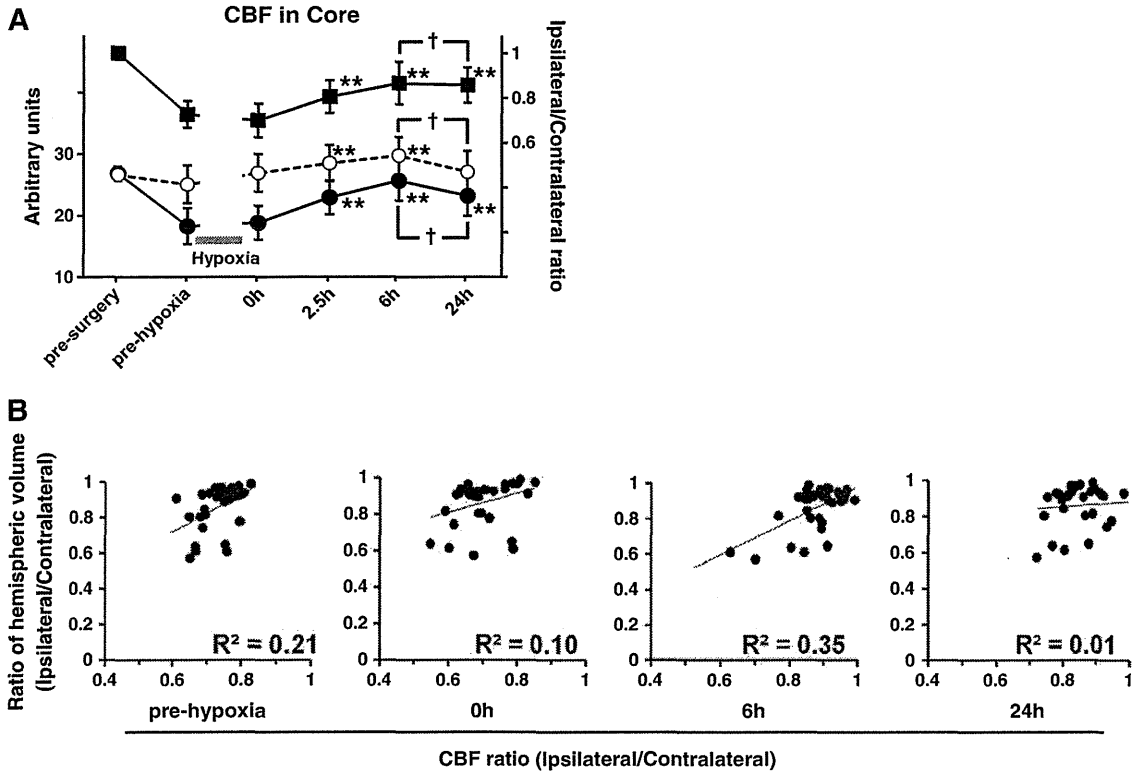

Fig. 6. (A) The temporal profile of CBF in the Core region in rat pups. The mean CBF in the ipsilateral hemisphere is significantly decreased after carotid artery ligation alone. After the hypoxic exposure, the mean CBF level is significantly increased at 2.5 h, 6 h, and 24 h of reperfusion, compared with its pre-hypoxia level. By contrast, the mean CBF in the contralateral hemisphere remains unchanged after carotid artery ligation alone. After the hypoxic exposure, the mean CBF level significantly increased at 2.5 h and 6 h, compared with the pre-hypoxia CBF level. $^{**}p<0.01$. The CBF level in each hemisphere is significantly decreased at 24 h, compared with its level at the 9 h. $\dagger p<0.05$. (B) The ratio of the ipsilateral CBF to contralateral CBF in the Core at each time point was compared with the ratio of the ipsilateral hemispheric volume to the contralateral hemispheric volume that was assessed seven days after the HI injury in the rats. The correlation between CBF and brain injury is significant and strongest at 6 h of reperfusion.

Discussion

Temporal profiles of CBF

In the present study, we demonstrated the spatial and temporal profiles of cortical surface CBF in mouse and rat pups. After carotid artery ligation alone, the mean CBF was decreased in the ipsilateral hemisphere in the mouse and rat pups. Following the hypoxic insult (i.e., with the initiation of reperfusion), the mean CBF on the ipsilateral side gradually increased; it nearly approached its pre-surgery level during the late reperfusion phase (at 9 h in mice and at 6 h in rats). It then decreased by 24 h.

In a classical study that used carbon-14 autoradiography in immature rats, blood flow to individual structures in the ipsilateral cerebral hemisphere was not affected by unilateral arterial occlusion alone (Vannucci et al., 1988). During the HI insult, the regional CBF of the ipsilateral hemisphere decreased. In a subsequent study, the researchers found that the CBF was similar in both hemispheres after 30 min, 4 h, and 24 h of recovery, and that the CBF did not differ from age-matched controls (Mujsce et al., 1990).

Most non-invasive studies measure CBF only until the early reperfusion phase; however, one LDF study measured CBF changes occurring from before surgery until 24 h after an HI injury in immature rodents (Wainwright et al., 2007). The CBF in the ipsilateral hemisphere was significantly decreased after carotid artery ligation alone and at 2 h after the HI insult, compared with the pre-surgery level. The CBF level then slowly returned to its pre-surgery level. On the other hand, the CBF in the contralateral hemisphere increased during reperfusion, before normalizing 24 h after the HI insult. Using the magnetic resonance arterial spin-labeling technique, Qiao et al. (2004) measured CBF prior to hypoxia, during hypoxia, and 1 h and 24 h after hypoxia in P7 rats with an HI injury. Following carotid artery occlusion and prior to hypoxic exposure, the cortical CBF levels were reduced, compared with the levels in the sham animals. At 1 h of reperfusion (i.e., after the cessation of hypoxia), the CBF approached levels close to the pre-hypoxic exposure levels. At 24 h of reperfusion, the CBF in the ipsilateral cortex further recovered, although the flow was still below that of the sham animals. These two reports are mostly in accordance with our data.

The apparent conflicting results of our study with studies using autoradiography may be because of the different techniques and regions used to measure CBF. We measured the CBF on the cortical surface, while the other researchers used coronal sections. The CBF was measured with a diffusible indicator in the other studies. A diffusible indicator is more representative of plasma flow (Mujsce et al., 1990), whereas LSF and LDF reflect red blood cell flow in the brain surface. Even among studies using the same CBF measuring techniques, there are conflicting reports.

The intensity of an HI insult may also explain the discrepancy of the reported data on CBF during reperfusion (Karlsson et al., 1994; Todd et al., 1986). Mild to moderate ischemia is followed by an initial period of hyperperfusion; a severe insult is followed by hypoperfusion (Fellman and Raivio, 1997). In adult rats with ischemia, it has been shown that the degree of postischemic hypoperfusion increases with increasing duration of ischemia, while the onset of postischemic hypoperfusion is delayed with increasing duration of ischemia. The mechanisms of hypoperfusion have been variously

ascribed to endothelial injury and swelling, to granulocytic plugging of microvessels, and to intravascular clotting (Fellman and Raivio, 1997).

The temporal profiles of CBF after an HI insult were similar in mice and rats, although there were some differences. Apart from species differences, differences in the intensity of the HI insult may have influenced the results. The degree of brain injury was more severe in the mice than in the rats, even though we had tried to optimize the duration of the hypoxic exposure to obtain a similar degree of brain injury, to obtain a similar percentage of pups with no obvious brain lesion, and to obtain a similar mortality rate in each species. Another factor that may have influenced the differences is that the CB17 mouse is a strain in which there are few variations in the MCA branches (Taguchi et al., 2010).

Predicting later brain injury by CBF and reducing animal variability

Animal models of ischemic disease show a heterogeneous degree of brain injury. This lesion variability is highlighted by animals that do not develop any lesion, despite proper surgical procedures. These animals with an intact brain are seen in HI models and in stroke models that use transient occlusion of the MCA (Derugin et al., 2000; Wendland et al., 2008) or that use permanent occlusion of the MCA (Bonnin et al., 2011) and carotid artery (Comi et al., 2005). To offset this animal variability, we examined CBF during reperfusion to see if it could be utilized as a predictive factor for later brain injury. The correlation between CBF and later brain injury was significant in mice ($R^2=0.89$) and in rats ($R^2=0.35$). The strong correlation in mice in the current study is remarkable when compared with other measures in literature. It is even stronger than the coefficient of determination for the cortex ($R^2=0.83$), which was assessed by MRI (using the 9.4T system) and Nissl-stained histology (Ten et al., 2004). MRI and histological examinations were performed at the same time point (i.e., 10 weeks after the HI insult). (In our study, the CBF was analyzed hours after the HI insult and a histological examination was performed seven days after the HI insult. The correlation is nevertheless stronger in our study than in the MRI study.) The present study interestingly demonstrated that the cortical surface CBF, as measured by LSF, was well correlated with later injury in deep brain structures, such as the hippocampus and thalamus.

We believe that CBF, as measured by LSF, can be used in preclinical research with rodents in two different ways. First, the LSF technique optimizes the extent of brain injury by excluding a portion of pups with no lesion or excluding pups with a massive lesion. Second, the LSF technique enables the analysis of the effect of an intervention on temporal and spatial changes in CBF, so that the mechanisms of neuroprotection (in relation to the CBF) can be assessed.

We examined how effectively pups with no brain lesion or minimal brain lesion can be excluded by using CBF analysis. In the present study, there were seven mouse pups with no lesion or a minimal lesion, which was defined as an ipsilateral/contralateral hemispheric volume ratio greater than 0.90. With the ipsilateral/contralateral Core CBF ratio cut-off value set at 0.78 at 24 h of reperfusion, nine pups out of 22 pups were excluded. Using this criterion, all seven mouse pups with no lesion or a minimal lesion were accurately excluded. (Therefore, the sensitivity was 100%; and the specificity, 87%). There were seven rat pups with no lesion or a minimal lesion. In rats, a minimal lesion was defined as an ipsilateral/contralateral hemispheric volume ratio greater than 0.95. With the ipsilateral/contralateral Core CBF ratio cut-off value set at 0.90 at 6 h of reperfusion, the sensitivity was 57% and specificity was 65% for excluding pups with no lesion or a minimal lesion.

A limitation of this method is that excluding pups with no lesion may not be practical at an early time point. Most therapeutic interventions tested in experimental models are administered either before or immediately after an HI insult. In the mice in the current study, the correlation between later brain injury and the Core CBF after reperfusion remained strong at 2.5 h ($R^2=0.36$) and at 6 h ($R^2=0.73$). However, the correlation at 0 h ($R^2=0.05$) and at 1 h ($R^2=0.15$) was weaker than at later time points, and therefore was not useful for predicting brain injury. This was the same trend noted in rats.

Cell therapies such as umbilical cord blood mononuclear cells or mesenchymal stem cells derived from bone marrow have recently been shown to be effective treatments in ischemic models (Taguchi et al., 2004; van Velthoven et al., 2010). The cells are administered days after a brain injury. Our method of using CBF to predict brain injury would be particularly useful in studies in which interventions such as cell therapy are administered some time after the brain injury.

The graph with linear regression in Fig. 5 shows that a relationship is evident between neuroprotection and CBF. A flattened slope of linear regression indicates that neuroprotection is independent of CBF. By contrast, when the line is unchanged and the data points shift toward the right upper side of the line, neuroprotection would be mainly the result of increased CBF after an intervention. In this way, the mechanisms of the intervention, in relation to the CBF, can be speculated. In the present study, a graph of the correlation between CBF and brain injury shows that dexamethasone treatment shifted the plots to the top (which indicates decreased brain injury), but the treatment did not shift the plots horizontally (which indicates no change in the CBF). This finding is in line with a previous study that used carbon-14 autoradiography and showed that dexamethasone prevented cerebral infarction without affecting the CBF during hypoxia in neonatal rats (Tuor et al., 1993). LSF can be used to test speculations concerning the mechanisms of an intervention, regardless of the timing of the intervention.

Derugin et al. (2000) used diffusion-weighted MRI (DWI) in a neonatal rat model with transient MCA occlusion to offset animal variability. DWI performed 24 h after reoxygenation, predicted the histological development of a lesion seven days after an ischemic insult in nine of 10 rats studied. They were not able to predict a lesion when DWI was performed 2 h after the initiation of reoxygenation. DWI did not detect a lesion in three rats at 2 h or at 24 h after the HI insult; however, one of these three rats developed a brain injury (Wendland et al., 2008).

Bonnin et al. (2011) used color-coded pulsed Doppler ultrasound imaging to assess CBF in a neonatal rat model that used permanent MCA occlusion with transient left common carotid artery occlusion. They measured the mean blood-flow velocity in the internal carotid arteries and the basilar trunk at three time points: before arterial occlusion, during the left common carotid artery occlusion, and 15 min after reperfusion. The mean blood-flow velocity during the transient occlusion showed a predictive value for brain injury. To our knowledge, there are no other reports demonstrating useful predictive parameters for brain injury after an HI insult in immature rodents. We believe that our LSF method is a useful and easy-to-perform way to predict later brain injury. By contrast, MRI is a time-consuming technique to perform, and color-coded pulsed Doppler ultrasound imaging may require trained hands, especially when examining immature rodents.

Clinical studies in CBF after HIE

The data of temporal changes in CBF in asphyxiated neonates during the first day of life are scarce and contradictory. Most studies using MRI, single photon emission tomography, or positron emission tomography assess CBF several days or weeks after birth (Rosenbaum et al., 1997).

In some studies, decreased CBF during reperfusion indicated a poor prognosis. One study used near-infrared spectroscopy (NIRS)

to assess changes in cerebral hemodynamics (van Bel et al., 1993). In neonates with an adverse outcome at one year of age, the cerebral blood volume had been decreased during the first 12 h of life (compared with the baseline value), suggesting a decrease in cerebral perfusion. Kirimi et al. (2002) used ultrasonography to assess the hemodynamic parameters of the MCA during the first 12 h of life in term neonates with HIE. The peak systolic velocity and the end diastolic velocity were significantly lower (and the resistive index was significantly higher) in neonates with a poor prognosis than in neonates with a good prognosis. By contrast, the cerebral blood volume was stable or increased during the first 12 h of life in infants with a normal one-year outcome.

In other studies, increased CBF during reperfusion indicated a poor prognosis. In asphyxiated term neonates, the global CBF during the first day of life was assessed by using the intravenous xenon 133 technique (Pryds et al., 1990). The mean CBF in infants with a poor prognosis was significantly higher than the mean CBF in infants with a good prognosis or in the control infants. Using Doppler ultrasonography, Ilves et al. (1998) assessed changes in CBF velocity in the major cranial arteries. Asphyxiated infants with a moderate stage of HIE had a significantly low CBF velocity (i.e., hypoperfusion) in the MCA at the age of 12 h. From the age of 24 h onward, there were no differences in the mean CBF velocity in these infants, compared with the CBF velocity in normal infants. Infants with a severe stage of HIE had a significantly high CBF velocity (i.e., hyperperfusion) in the MCA from the age of 12 h onwards. All of the infants that had a severe stage of HIE and a markedly high mean CBF velocity at the age of 12 h either died or developed multicystic degeneration of the brain.

Conclusions

Our major finding is that the degree of the CBF during the late reperfusion phase is strongly associated with the extent of later morphological brain damage. Using LSF to analyze CBF reduces animal variability, thereby reducing the number of animals that need to be used. Conflicting results in reports suggest that hemodynamic responses to an HI insult are sensitive to the severity and the duration of the insult; the time points and regions measured; and the strains and species of animals used. Because of this sensitivity, an easy and repeatable technique is crucial in assessing the CBF in animals with an HI insult. We believe that our LSF method is useful for studies using immature rodents with an HI insult and stroke. We also believe that this method would make detailed analyses possible.

Disclosure/conflict of interest

None

Sources of funding

This work was supported by a Grant-in-Aid for Scientific Research (JSPS KAKENHI 22890254) from the Ministry of Education, Culture, Sports, Science and Technology of Japan.

Acknowledgments

We thank Manami Sone for excellent technical assistance with histological preparations, Akiko Kada for statistical assistance.

References

Ayata, C., Dunn, A.K., Gursoy, O.Y., Huang, Z., Boas, D.A., Moskowitz, M.A., 2004. Laser speckle flowmetry for the study of cerebrovascular physiology in normal and ischemic mouse cortex. J. Cereb. Blood Flow Metab. 24, 744–755.

Bonnin, P., Leger, P.L., Deroide, N., Fau, S., Baud, O., Pocard, M., et al., 2011. Impact of intracranial blood-flow redistribution on stroke size during ischemia-reperfusion in 7-day-old rats. J. Neurosci. Methods 198, 103–109.

Comi, A.M., Johnston, M.V., Wilson, M.A., 2005. Strain variability, injury distribution, and seizure onset in a mouse model of stroke in the immature brain. Dev. Neurosci. 27, 127–133.

Derugin, N., Wendland, M., Muramatsu, K., Roberts, T.P., Gregory, G., Ferriero, D.M., et al., 2000. Evolution of brain injury after transient middle cerebral artery occlusion in neonatal rats. Stroke 31, 1752–1761.

Dunn, A.K., Bolay, H., Moskowitz, M.A., Boas, D.A., 2001. Dynamic imaging of cerebral blood flow using laser speckle. J. Cereb. Blood Flow Metab. 21, 195–201.

Fabian, R.H., Perez-Polo, J.R., Kent, T.A., 2008. Perivascular nitric oxide and superoxide in neonatal cerebral hypoxia–ischemia. Am. J. Physiol. Heart Circ. Physiol. 295, H1809–H1814.

Fellman, V., Raivio, K.O., 1997. Reperfusion injury as the mechanism of brain damage after perinatal asphyxia. Pediatr. Res. 41, 599–606.

Forrester, K.R., Stewart, C., Tulip, J., Leonard, C., Bray, R.C., 2002. Comparison of laser speckle and laser doppler perfusion imaging: measurement in human skin and rabbit articular tissue. Med. Biol. Eng. Comput. 40, 687–697.

Fujita, Y., Ihara, M., Ushiki, T., Hirai, H., Kizaka-Kondoh, S., Hiraoka, M., et al., 2010. Early protective effect of bone marrow mononuclear cells against ischemic white matter damage through augmentation of cerebral blood flow. Stroke 41, 2938–2943.

Ilves, P., Talvik, R., Talvik, T., 1998. Changes in Doppler ultrasonography in asphyxiated term infants with hypoxic–ischaemic encephalopathy. Acta Paediatr. 87, 680–684.

Ioroi, T., Yonetani, M., Nakamura, H., 1998. Effects of hypoxia and reoxygenation on nitric oxide production and cerebral blood flow in developing rat striatum. Pediatr. Res. 43, 733–737.

Johnston, M.V., Ferriero, D.M., Vannucci, S.J., Hagberg, H., 2005. Models of cerebral palsy: which ones are best? J. Child Neurol. 20, 984–987.

Karlsson, B.R., Grogaard, B., Gerdin, B., Steen, P.A., 1994. The severity of postischemic hypoperfusion increases with duration of cerebral ischemia in rats. Acta Anaesthesiol. Scand. 38, 248–253.

Kirimi, E., Tuncer, O., Atas, B., Sakarya, M.E., Ceylan, A., 2002. Clinical value of color doppler ultrasonography measurements of full-term newborns with perinatal asphyxia and hypoxic ischemic encephalopathy in the first 12 hours of life and long-term prognosis. Tohoku J. Exp. Med. 197, 27–33.

Lindström, K., Lagerroos, P., Gillberg, C., Fernell, E., 2006. Teenage outcome after being born at term with moderate neonatal encephalopathy. Pediatr. Neurol. 35, 268–274.

Liu, X.H., Kwon, D., Schielke, G.P., Yang, G.Y., Silverstein, F.S., Barks, J.D., 1999. Mice deficient in interleukin-1 converting enzyme are resistant to neonatal hypoxic–ischemic brain damage. J. Cereb. Blood Flow Metab. 19, 1099–1108.

Matsiukevich, D., Randis, T.M., Utkina-Sosunova, I., Polin, R.A., Ten, V.S., 2010. The state of systemic circulation, collapsed or preserved defines the need for hyperoxic or normoxic resuscitation in neonatal mice with hypoxia–ischemia. Resuscitation 81, 224–229.

Mujsce, D.J., Christensen, M.A., Vannucci, R.C., 1990. Cerebral blood flow and edema in perinatal hypoxic–ischemic brain damage. Pediatr. Res. 27, 450–453.

Pryds, O., Greisen, G., Lou, H., Friis-Hansen, B., 1990. Vasoparalysis associated with brain damage in asphyxiated term infants. J. Pediatr. 117, 119–125.

Qiao, M., Latta, P., Foniok, T., Buist, R., Meng, S., Tomanek, B., et al., 2004. Cerebral blood flow response to a hypoxic–ischemic insult differs in neonatal and juvenile rats. MAGMA 17, 117–124.

Rice III, J.E., Vannucci, R.C., Brierley, J.B., 1981. The influence of immaturity on hypoxic–ischemic brain damage in the rat. Ann. Neurol. 9, 131–141.

Ringel, M., Bryan, R.M., Vannucci, R.C., 1991. Regional cerebral blood flow during hypoxia–ischemia in the immature rat: comparison of iodoantipyrine and iodoamphetamine as radioactive tracers. Brain Res. Dev. Brain Res. 59, 231–235.

Riyamongkol, P., Zhao, W., Liu, Y., Belayev, L., Busto, R., Ginsberg, M.D., 2002. Automated registration of laser Doppler perfusion images by an adaptive correlation approach: application to focal cerebral ischemia in the rat. J. Neurosci. Methods 122, 79–90.

Rosenbaum, J.L., Almli, C.R., Yundt, K.D., Altman, D.I., Powers, W.J., 1997. Higher neonatal cerebral blood flow correlates with worse childhood neurologic outcome. Neurology 49, 1035–1041.

Sheldon, R.A., Sedik, C., Ferriero, D.M., 1998. Strain-related brain injury in neonatal mice subjected to hypoxia–ischemia. Brain Res. 810, 114–122.

Stern, M.D., Lappe, D.L., Bowen, P.D., Chimosky, J.E., Holloway Jr., G.A., Keiser, H.R., et al., 1977. Continuous measurement of tissue blood flow by laser-Doppler spectroscopy. Am. J. Physiol. 232, H441–H448.

Strong, A.J., Bezzina, E.L., Anderson, P.J., Boutelle, M.G., Hopwood, S.E., Dunn, A.K., 2006. Evaluation of laser speckle flowmetry for imaging cortical perfusion in experimental stroke studies: quantitation of perfusion and detection of peri-infarct depolarisations. J. Cereb. Blood Flow Metab. 26, 645–653.

Taguchi, A., Soma, T., Tanaka, H., Kanda, T., Nishimura, H., Yoshikawa, H., et al., 2004. Administration of CD34+ cells after stroke enhances neurogenesis via angiogenesis in a mouse model. J. Clin. Invest. 114, 330–338.

Taguchi, A., Kasahara, Y., Nakagomi, T., Stern, D.M., Fukunaga, M., Ishikawa, M., et al., 2010. A reproducible and simple model of permanent cerebral ischemia in CB-17 and SCID mice. J. Exp. Stroke Transl. Med. 3, 28–33.

Taniguchi, H., Mohri, I., Okabe-Arahori, H., Aritake, K., Wada, K., Kanekiyo, T., et al., 2007. Prostaglandin D2 protects neonatal mouse brain from hypoxic ischemic injury. J. Neurosci. 27, 4303–4312.

Ten, V.S., Wu, E.X., Tang, H., Bradley-Moore, M., Fedarau, M.V., Ratner, V.I., et al., 2004. Late measures of brain injury after neonatal hypoxia–ischemia in mice. Stroke 35, 2183–2188.

Todd, N.V., Picozzi, P., Crockard, H.A., Russell, R.R., 1986. Reperfusion after cerebral ischemia: influence of duration of ischemia. Stroke 17, 460–466.

Tsuji, M., Wilson, M.A., Lange, M.S., Johnston, M.V., 2004. Minocycline worsens hypoxic–ischemic brain injury in a neonatal mouse model. Exp. Neurol. 189, 58–65.

Tuor, U.I., 1995. Dexamethasone and the prevention of neonatal hypoxic–ischemic brain damage. Ann. N. Y. Acad. Sci. 765, 179–195.
Tuor, U.I., Simone, C.S., Barks, J.D., Post, M., 1993. Dexamethasone prevents cerebral infarction without affecting cerebral blood flow in neonatal rats. Stroke 24, 452–457.
van Bel, F., Dorrepaal, C.A., Benders, M.J., Zeeuwe, P.E., van de Bor, M., Berger, H.M., 1993. Changes in cerebral hemodynamics and oxygenation in the first 24 hours after birth asphyxia. Pediatrics 92, 365–372.
van Handel, M., Swaab, H., de Vries, L.S., Jongmans, M.J., 2007. Long-term cognitive and behavioral consequences of neonatal encephalopathy following perinatal asphyxia: a review. Eur. J. Pediatr. 166, 645–654.
van Velthoven, C.T., Kavelaars, A., van Bel, F., Heijnen, C.J., 2010. Nasal administration of stem cells: a promising novel route to treat neonatal ischemic brain damage. Pediatr. Res. 68, 419–422.
Vannucci, R.C., Lyons, D.T., Vasta, F., 1988. Regional cerebral blood flow during hypoxia–ischemia in immature rats. Stroke 19, 245–250.
Wainwright, M.S., Grundhoefer, D., Sharma, S., Black, S.M., 2007. A nitric oxide donor reduces brain injury and enhances recovery of cerebral blood flow after hypoxia–ischemia in the newborn rat. Neurosci. Lett. 415, 124–129.
Wendland, M.F., Faustino, J., West, T., Manabat, C., Holtzman, D.M., Vexler, Z.S., 2008. Early diffusion-weighted MRI as a predictor of caspase-3 activation after hypoxic–ischemic insult in neonatal rodents. Stroke 39, 1862–1868.

Cilostazol Reduces the Risk of Hemorrhagic Infarction After Administration of Tissue-Type Plasminogen Activator in a Murine Stroke Model

Yukiko Kasahara; Takayuki Nakagomi, MD; Tomohiro Matsuyama, MD; David Stern, MD; Akihiko Taguchi, MD

Background and Purpose—Prior use of antiplatelet agents improves stroke outcome in patients undergoing thrombolytic therapy as shown by reduced arterial reocclusion, although the risk of cerebral hemorrhage can be increased.

Methods—The effect of cilostazol, an antiplatelet drug that improves endothelial function through upregulation of intracellular cAMP, on cerebral hemorrhage after thrombolytic therapy was investigated using a highly reproducible transient ischemia model.

Results—Treatment with cilostazol for 7 days before ischemia significantly suppressed the risk and severity of cerebral hemorrhage after injection of tissue-type plasminogen activator, although treatment with aspirin had no such protective effect compared with nontreated mice. Immunohistological analysis revealed that treatment with cilostazol suppressed disruption of the microvasculature in the ischemic area associated with reduced matrix metalloproteinase-9 activity.

Conclusions—Our results suggest that patients treated with cilostazol before onset of stroke could have a lower risk of cerebral hemorrhage after thrombolytic therapy and might also have a longer therapeutic time window for thrombolysis. Furthermore, the risk of cerebral hemorrhage can be significantly altered by prestroke therapies, and analysis of the effects of multiple drugs on tissue-type plasminogen activator-induced cerebral hemorrhage in animal models is essential for the extending safe and effective thrombolytic therapy to a wider group of patients. **(*Stroke*. 2012;43:499-506.)**

Key Words: antiplatelet drugs ■ brain ischemia ■ ICH ■ murine model ■ thrombolysis

Intravenous thrombolysis with tissue-type plasminogen activator (tPA) has been shown to improve functional outcomes of patients with stroke when given within 3 hours from the onset of stroke.[1,2] However, treatment with tPA significantly increases the risk of bleeding events, including hemorrhagic infarction.[3,4] Although a number of clinical studies indicate that prior use of antiplatelet agents increases the risk of cerebral hemorrhage after thrombolytic therapy,[5–7] the use of antiplatelet agents had been shown to improve stroke outcome compared with patients without such therapy.[8,9] The beneficial effects of antiplatelet drugs may be attributed to improved microcirculatory function and diminished reocclusion after tPA treatment, the latter observed in 20% to 34% of patients after initially successful recanalization.[10,11] Reocclusion after tPA treatment is induced, at least in part, by the activation of the coagulation cascade by tPA.[12,13] These findings indicate that the use of antiplatelet drugs is potentially a double-edged sword in the context of tPA treatment; that is, use of antiplatelet agents is likely to be beneficial for stroke outcome despite increased risk of hemorrhagic infarction. Consistent with these findings, a randomized controlled trial in the Netherlands has shown that thrombolysis in combination with antiplatelet drugs prevented reocclusion and improved the clinical outcome.[14]

Recently, cilostazol, an antiplatelet drug that inhibits the activity of cAMP phosphodiesterase Type 3, has been shown to be superior to aspirin for secondary prevention of stroke with fewer hemorrhagic events.[15] Compared with other antiplatelet drugs, cilostazol is known to have milder hemorrhagic side effects[16] and prevent the increase in bleeding time.[17] In this study, we focused on cilostazol and investigated its effect on hemorrhagic infarction after treatment with tPA using a murine ischemia–reperfusion model.

Materials and Methods

All procedures were performed under the auspices of an approved protocol of the National Cerebral and Cardiovascular Center Animal Care and Use Committee.

Received August 9, 2011; final revision received September 12, 2011; accepted September 29, 2011.

Miguel Perez-Pinzon, PhD, was the Guest Editor for this paper.

From the Department of Cerebrovascular Disease (Y.K., A.T.), National Cerebral and Cardiovascular Center, Osaka, Japan; the Institute for Advanced Medical Sciences (T.N., T.M.), Hyogo College of Medicine, Hyogo, Japan; and the Executive Dean's Office (D.S.), University of Tennessee, Knoxville, TN.

Correspondence to Akihiko Taguchi, MD, Department of Cerebrovascular Disease, National Cerebral and Cardiovascular Center, 5-7-1 Fujishiro-dai, Suita, Osaka, Japan, 565-8565. E-mail taguchi@ri.ncvc.go.jp

Stroke **is available at http://stroke.ahajournals.org** **DOI: 10.1161/STROKEAHA.111.635417**

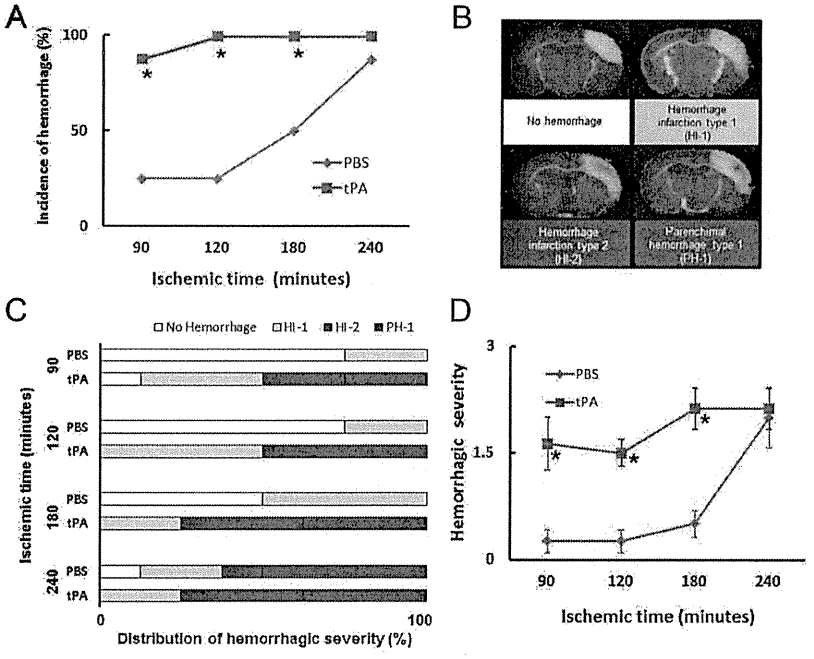

Figure 1. Administration of tPA and hemorrhagic infarction after transient ischemia. **A,** Administration of tPA at 90, 120, and 180 minutes after transient ischemia significantly increased the risk of cerebral hemorrhage compared with controls treated with PBS. **B,** Severity of cerebral hemorrhage was scored according to its type and extension by blinded investigator. Representative photographs of each hemorrhagic severity are shown. **C–D,** Distribution of each hemorrhagic severity is shown in **C.** Quantitative analysis revealed increased severity of cerebral hemorrhage with injection of tPA at 90, 120, and 180 minutes after ischemia compared with PBS injection (**D**). * $P<0.05$ vs PBS control (**A, D**). N=8, in each group. tPA indicates tissue-type plasminogen activator; PBS, phosphate-buffered saline.

Induction of Focal Cerebral Ischemia

To evaluate the effect of cilostazol on tPA-induced hemorrhagic infarction, we developed a highly reproducible murine transient cerebral ischemia model based on modification of our previous method.[18] In brief, the left middle cerebral artery (MCA) was isolated in male 7-week-old CB17/Icr mice (Clea, Tokyo, Japan) under halothane inhalation (3%) anesthesia and transient focal cerebral ischemia was induced under direct vision by transiently occluding the distal portion of the left MCA with a monofilament nylon suture (7-0 in size; Tyco) for 90, 120, 180, or 240 minutes. During surgical procedures, rectal temperature was monitored and controlled at 37.0±0.2°C by a feedback-regulated heating pad. Cerebral blood flow in the MCA area was monitored as described.[19] All mice showed a >75% decrease in cerebral blood flow rapidly after occlusion and restored cerebral blood flow (>0%) soon after reperfusion compared with before transient ligation of the MCA. tPA (10 mg/kg body weight in 0.1 mL saline; Mitsubishi Tanabe Pharmaceutical Co, Tokyo, Japan) was infused through the tail vein just before reperfusion. In sham-operated controls, the same procedure was used and intravenous saline (same volume) was injected in place of tPA.

Drug Administration

Mice were fed cilostazol (0.3% in the diet; Otsuka, Tokushima, Japan), aspirin (0.1% in the diet; Eizai, Tokyo, Japan), or a normal diet for 7 days before induction of ischemia. Doses of cilostazol and aspirin were determined according to previous reports.[20–22] tPA (10 mg/kg) was administered through the tail vein just before reperfusion. The dose of tPA was determined according to previous reports.[23,24]

Assessment of Hemorrhage and Infarction

Hemorrhagic infarction was evaluated at 24 hours after induction of ischemia as described previously.[25,26] Briefly, coronal forebrain sections (1 mm thick) were stained with 1% 2,3,5-triphenyltetrazolium (Sigma-Aldrich, St. Louis, MO) for 20 minutes at 37°C and fixed in 4% paraformaldehyde/phosphate-buffered saline (PBS; pH 7.4). Infarct volume was measured using a microscopic digital camera system (Olympus, Tokyo, Japan) as described previously.[27] Briefly, the 2,3,5-triphenyltetrazolium-positive area of each hemisphere was estimated using National Institutes of Health Image software (Version 1.62), and volume of the surviving/viable tissue was calculated by integrating the overall coronally oriented area. Percent stroke volume was evaluated by [(contralateral hemisphere volume)−(infarcted hemisphere volume)]/[(contralateral hemisphere volume)×2]×100%.

The severity of cerebral hemorrhage was quantified by investigators who were not informed regarding the experimental protocol and identity of samples under study, as described previously[28,29]: nonhemorrhage (Score 0); hemorrhagic infarction Type 1 (HI-1), defined as heterogeneous small petechiae, generally along the boundary of the infarct (Score 1); hemorrhagic infarction Type 2 (HI-2), with more confluent petechiae within the infarcted area (Score 2); parenchymal hemorrhage Type 1 (PH-1), characterized by hematoma covering <30% of the injured parenchyma (Score 3); and parenchymal hemorrhage Type 2 (PH-2) with dense hematoma in >30% of the infarct (Score 4). Examples of each score are demonstrated in Figure 1B (no mouse showed PH-2 in our experiment).

Immunohistochemistry

Twenty-four hours after reperfusion, mice were deeply anesthetized with sodium pentobarbital and perfused transcardially with saline followed by 4% paraformaldehyde. Forebrain coronal sections (20 μm) were prepared using a vibroslicer (Leica, Wetzlar, Germany) and immunostained with antibodies to platelet endothelial cell adhesion molecule 1 (PECAM-1; BD Pharmingen, San Jose, CA; dilution 1:500), lectin (Invitrogen, Carlsbad, CA; 1:50), and matrix metalloproteinase (MMP)-9 (Santa Cruz Biotechnology, Santa Cruz, CA; dilution 1:100) using standard immunohistochemical procedures. Anti-PECAM-1 and lectin were visualized by the 3,3′-diaminobenzidine method. Alexa488 or Alexa555 antibody was used as the secondary antibody for anti-MMP-9 and PECAM-1. Vascular density was evaluated using anti-PECAM-1 antibody as described previously.[27]

Briefly, the number of PECAM-1-positive vascular structures in the anterior cerebral artery area (border of cerebral ischemia; approximately 0.5 mm from the border of infarction), MCA area (stroke area), and contralateral cortex at the exact center of the forebrain section was counted by investigators who were not informed regarding the experimental protocol and identity of samples under study (3 random fields in each section were scored and the area of each field was 0.12 mm^2). Sections stained with antilectin

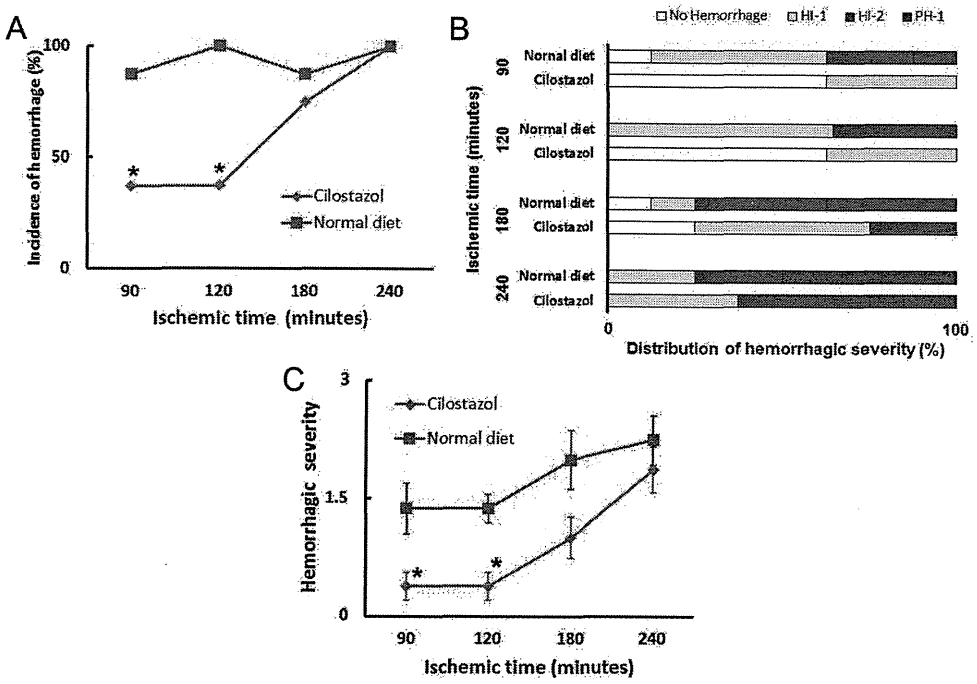

Figure 2. Administration of cilostazol reduced the risk of cerebral hemorrhage after tPA treatment. **A**, Mice fed a cilostazol-containing diet for 7 days before ischemia showed significantly reduced risk of cerebral hemorrhage after 90 and 120 minutes ischemia with tPA injection compared with mice fed a normal diet. **B–C**, The distribution of each hemorrhagic severity is shown in **B**. Quantitative analysis revealed reduced severity of cerebral hemorrhage in mice fed cilostazol after 90 and 120 minutes of ischemia with tPA injection compared with mice fed a normal diet (**C**). *$P<0.05$ vs normal diet control (**A, C**). N=8, in each group. tPA indicates tissue-type plasminogen activator.

were counterstained with Mayer hematoxylin solution (Wako, Osaka, Japan).

Gelatin Zymography

The level of MMP-9 in the ischemic brain was evaluated by gelatin zymography, as described previously.[23] Briefly, at 24 hours after reperfusion with injection of tPA, brain tissue from the ipsilateral ischemic and contralateral nonischemic hemispheres was removed and homogenized in lysis buffer (CelLytic MT; Sigma). After centrifugation at 500 g for 10 minutes, supernatant was collected and protein concentrations were measured by the Bradford assay (Bio-Rad). Protein samples (35 $\mu g/\mu L$) were mixed with 2× zymogram sample buffer (TEFCO, Tokyo, Japan) and loaded onto 10% Zymogram-PAGE mini (TEFCO). After electrophoresis, the gel was stained with Coomassie blue R-250 according to the manufacturer's protocol (ZYMOGRAM buffer kit; TEFCO). Gel images were captured using a digital camera (Olympus, Tokyo, Japan) with reversed brightness, and the intensity of each band was quantified with National Institutes of Health Image.

Data Analysis

Statistical comparisons among groups were determined using the Kruskal-Wallis test to compare with controls. Data are expressed as mean±SE.

Results

Administration of tPA Increases the Risk of Cerebral Hemorrhage After Transient Ischemia

To confirm the increased risk of cerebral hemorrhage after administration of tPA, transient ischemia was induced and tPA or PBS was injected just before reperfusion. The incidence and degree of hemorrhagic infarction were evaluated at 24 hours after reperfusion. As shown in Figure 1A, the incidence of hemorrhagic infarction was significantly increased with tPA injection after 90, 120, and 180 minutes of transient ischemia, although no significant increase was observed after 240 minutes ischemia. To investigate the severity of hemorrhagic infarction, degrees of hemorrhage were scored according to 5 subtypes, as described previously.[28,29] In our experimental groups, no mice showed PH-2 (Grade 4). Representative photographs of hemorrhage subtypes are shown in Figure 1B. It is notable that none of the mice that received PBS before reperfusion showed parenchymal hematoma (Grade ≥2) after 90, 120, and 180 minutes transient ischemia (Figure 1C). In contrast, mice receiving tPA showed PH even after 90 minutes ischemia. In both treatment groups, more than half of the mice showed PH after 240 minutes ischemia. Quantitative analysis revealed a significant increase in hemorrhagic score in mice treated with tPA at 90, 120, and 180 minutes after transient ischemia compared with PBS-treated groups (Figure 1D). The volume of infarcted tissue at 24 hours, consequent to 90 minutes ischemia to induce stroke, was evaluated. There was no significant difference in percent stroke volume between treatment with tPA and PBS (13.8%±1.1% and 13.7%±0.8%, respectively; $P=0.96$).

Cilostazol Reduced the Risk of tPA-Induced Cerebral Hemorrhage

To evaluate the risk of cilostazol on tPA-induced cerebral hemorrhage, mice were fed cilostazol for 7 days and transient ischemia was induced followed by injection of tPA. Contrary

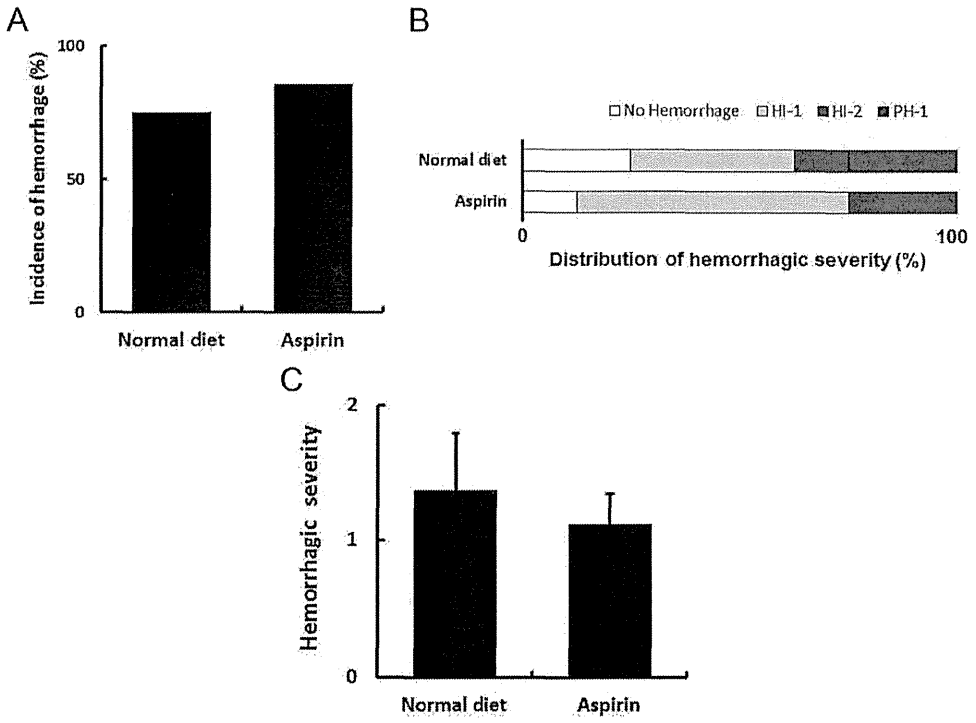

Figure 3. Aspirin administration did not alter the risk of cerebral hemorrhage after tPA treatment. **A**, Mice fed an aspirin-containing diet for 7 days before ischemia did not show a significant change in the risk of cerebral hemorrhage after 90 minutes of ischemia and tPA injection compared with mice fed a normal diet. **B–C**, Distribution of each hemorrhagic severity is shown in **B**. Quantitative analysis revealed no significant difference in the severity of cerebral hemorrhage between mice fed aspirin and the normal diet (**C**). N=8, in each group. tPA indicates tissue-type plasminogen activator.

to our initial expectation, the incidence of cerebral hemorrhage was significantly reduced on administration of cilostazol in mice after 90 and 120 minutes of transient ischemia, although no significant difference was observed after 180 and 240 minutes (Figure 2A). Figure 2B shows the distribution of severity in each group. It is notable that all of the mice fed cilostazol before injection of tPA showed no or mild hemorrhage (score 0 or 1) after 90 or 120 minutes ischemia. Quantitative analysis using the hemorrhagic score revealed a significant reduction of severity in mice pretreated with cilostazol at 90 and 120 minutes after transient ischemia compared with the nontreated group (Figure 2C). However, no statistical difference in the severity was observed between groups after 180 or 240 minutes of transient ischemia.

Aspirin Did Not Reduce the Risk of tPA-Induced Cerebral Hemorrhage

Aspirin is known to increase the risk of cerebral hemorrhage.[5,9,30] To investigate its effect on tPA-induced cerebral hemorrhage, mice were treated with aspirin for 1 week and transient ischemia was induced (90 minutes). The results displayed no significant reduction or increase in the incidence of cerebral hemorrhage on treatment with aspirin compared with normal controls (Figure 3A). Analysis of severity using the hemorrhagic score also revealed no significant change between the aspirin-treated and normal diet groups (Figure 3B–C). Although the incidence of hemorrhage was dependent on the time to reperfusion, these results indicate that aspirin has a nonsignificant effect on reduction of tPA-induced cerebral hemorrhage after 90 minutes of transient ischemia, whereas cilostazol had significant protective effects.

Cilostazol Prevented the Degradation of Cerebrovasculature After Transient Ischemia and Administration of tPA

To investigate mechanisms underlying the protective effect of cilostazol pretreatment on cerebral hemorrhage, morphological changes in cerebromicrovasculature were investigated at 24 hours after induction of transient ischemia (90 minutes). Immunohistological analysis revealed a decrease in PECAM-1-positive microvasculature at the border of cerebral ischemia after transient ischemia with tPA injection compared with the contralateral cortex (Figure 4A, contralateral; Figure 4B; ipsilateral). In contrast, pretreatment with cilostazol prevented the reduction in PECAM-1-positive microvasculature (Figure 4C). These impressions were confirmed by quantitative analysis of PECAM-1-positive vascular density (Figure 4D). PECAM-1 is known to be important for survival, migration, and functional organization of endothelial cells,[31] and our data indicate a beneficial effect of cilostazol on the preservation of these endothelial functions at the border of the stroke. In contrast, pretreatment with aspirin had no effect on the preservation of microvasculature (Figure 4E–F).

Next, we investigated possible degradation of cerebrovasculature in the stroke area with antilectin antibody, a marker of vascular morphology.[27] At 24 hours after transient ischemia (90 minutes) with tPA injection, a marked dissociation of microvasculature was observed in the ischemic brain in mice